Conservative finite-volume forms of the Saint-Venant equations for hydrology and urban drainage

Ben R. Hodges[1]

[1]National Center for Infrastructure Modeling and Management, University of Texas at Austin

Correspondence: hodges@utexas.edu

Abstract. New integral, finite-volume forms of the Saint-Venant equations for one-dimensional (1D) open-channel flow are derived. The new equations are in the flux-gradient conservation form and transfers portions of both the hydrostatic pressure force and the gravitational force from the source term to the conservative flux term. This approach prevents irregular channel topography from creating an inherently non-smooth source term for momentum. The derivation introduces an analytical approximation of the free surface across a finite volume element (e.g., linear, parabolic) with a weighting function for quadrature with bottom topography. This new free-surface/topography approach provides a single term that approximates the integrated piezometric pressure across a control volume that can be split between the source and the conservative flux terms without introducing new variables within the discretization. The resulting conservative finite-volume equations are written entirely in terms of flow rates, cross-sectional areas and water surface elevations – *without* using the bottom slope (S_0). The new Saint-Venant equation form is: (1) inherently conservative, as compared to non-conservative finite-difference forms, and (2) inherently "well-balanced" for irregular topography, as compared to conservative finite-volume forms using the Cunge-Liggett approach that rely on two integrations of topography. It is likely that this new equation form will be more tractable for large-scale simulations of river networks and urban drainage systems with highly-variable topography as it ensures the inhomogeneous source term of the momentum conservation equation is Lipschitz smooth as long as the solution variables are smooth.

1 Introduction

The one-dimensional Saint-Venant equations (SVE) are the simplest equations that capture the full dynamics of river and open-channel flow, and yet they are not universally used where river networks are explicitly represented in hydrological and urban drainage models. Furthermore, where the SVE are used the numerical solution methods typically employ a "non-conservative" form, which inherently has greater numerical dissipation than the "conservative" form. But even the undesirable non-conservative form of the SVE is little-used for large systems – instead, reduced-physics models are common. These approaches *a priori* neglect part some part of the flow dynamics for simpler computation (see Sections 2 and 3 for discussions of these issues). In their call for "hyperresolution global land surface modeling," Wood et al. (2011) postulated that the principle

issues that limit SVE use in river networks could be resolved by application of more computing power and more precise river geometry. Hodges (2013) argued that there were wider challenges to using the SVE, but these are not sufficient reasons relying on reduced physics models that are calibrated to get the "right answer for the wrong reason." In the intervening years some progress has been made toward improving applications of the SVE, but large-scale hydrological modeling of river networks with application of supercomputer power (e.g., the US National Water Model, Cohen et al., 2018) continues to rely on reduced-physics methods. Arguably, the dynamics of river flow are the most observable and should be the easiest part of hydrology to model (or at least with lower uncertainty in boundaries and forcing compared to the landscape), so it is unsatisfactory that more than 50 years after Preissmann (1961) we still are not universally using the SVE in hydrological modeling of river networks.

The present work evolved out of a frustration with the slow pace of improvement in SVE modeling. Taking a step backwards, we can ask – *is there something fundamental in the common forms of the SVE that hinders progress?* Motivated by an analysis of the equation forms (Section 2) and a study of the wealth of past work in the SVE (Section 3), new insights were developed and are presented herein. The fundamental theses of the present work are (1) conservative formulation of equations should be used for the next generation of river network models, and (2) the appearance of the channel slope (S_0) in the SVE for channels with irregular topography is a principle cause of instabilities and extended computational time. Neither thesis can be demonstrated herein – this work is merely a first step that provides the theoretical foundations for a conservative and inherently "well-balanced" approach that highlights the minimal level of approximations needed for an SVE form with irregular topography. It remains for future studies to compare models built on these foundations to the existing approaches to determine if the new forms provide significant numerical advantages.

The new conservative form of the SVE is developed with a goal of addressing challenges associated with modeling large-scale 1D flow network systems. In the process of developing the new form, we will encounter a philosophical question as to whether the primary vertical variable in a large-scale network solution should be the depth (H) or the water surface elevation (η). Despite our prior work with H primacy (Liu and Hodges, 2014), we shall see that there are advantages to using η as it is identical to the piezometric pressure, which is uniform over a channel cross-sectional area. The new derivation herein provides interesting possibilities for analytically including hyperresolution bathymetric knowledge while retaining larger computational elements for large-scale modeling. The interaction of subgrid-scale topography with subgrid free-surface gradients is handled in a new integrated piezometric pressure term that arises in the derivation. This idea is not fully exploited within the present work, but the framework is developed for others to build upon.

In the remainder of this paper, Section 2 provides motivation and context in the differential forms of the SVE. Section 3 provides a further overview of SVE modeling in the wide range of conservative and non-conservative forms. A new and complete derivation of the finite-volume form of the conservative 1D momentum equation with minimal approximations is provided in Section 4. Approximate forms of the 1D SVE are presented in Section 5, and the final form of the equations and a discussion of their potential use is provided Section 6.

2 Motivation

In reach-scale hydraulic studies, the Saint-Venant equations are almost always solved in a conservative form (e.g., Karelsky et al., 2000; Lai et al., 2002; Papanicolaou et al., 2004; Sanders, 2001), but usually in non-conservative form when used in river-network hydrology and urban drainage networks (e.g., Liu and Hodges, 2014; Pramanik et al., 2010; Rossman, 2017; Saleh et al., 2013). Arguably, the reasons are in the difficulty in obtaining a "well-balanced" model for the conservative form and the inherent complexities/uncertainties of channel geometry across a large network (see discussion in Section 3). In general, conservative equation forms are valued as they ensure (with careful discretization) that transport modeling does not numerically create or destroy the transported variable. Indeed, the use of the conservative form for mass conservation is universal in models from hydraulics to hydrology – it is only for momentum that the non-conservative form remains common.

To set the context for this paper, consider the non-conservative form of momentum that has been used in large network solutions (Liu and Hodges, 2014)

$$\frac{\partial Q}{dt}+\frac{\partial}{\partial x}\left(\beta\frac{Q^2}{A}\right)+gA\frac{\partial H}{\partial x}=gA\left(S_0-S_f\right) \tag{1}$$

where Q is the flow rate, A is the channel cross-sectional area, β is the momentum coefficient (associated with non-uniform velocities integrated over A), g is gravity, H is the water depth, S_0 is the channel slope, and S_f is the friction slope. The above equation has immediate physical appeal as each term represents a clearly understood piece of physics; i.e., the rate of change of the flow is affected by the gradient of nonlinear advection, the hydrostatic pressure gradient (driven by water depth), the gravitational force along the slope, and frictional resistance. The equation includes a conservative form of nonlinear advection (all the variables inside the gradient), but $gA\partial H/\partial x$ is non-conservative (that is A, which is a function of H, is outside the gradient). The terms to the right-hand-side (RHS) of the equal sign are considered source terms that inherently lead to non-conservation of momentum. Thus, a "conservative" form of the above could be formally written as

$$\frac{\partial Q}{dt}+\frac{\partial}{\partial x}\left(\beta\frac{Q^2}{A}\right)=-gA\frac{\partial H}{\partial x}+gA\left(S_0-S_f\right) \tag{2}$$

where the trivial act of moving the pressure gradient term to the RHS is a recognition that it can cause non-conservation (source/sink) of the conserved momentum fluxes from the left-hand-side (LHS). That is, any component on the RHS is capable of creating or destroying momentum whereas the terms on the LHS (if properly discretized) cannot. Eq. (2) is not particularly common as a conservative form, but is sometimes seen (Ying et al., 2004; Wu and Wang, 2007; Ying and Wang, 2008). The above equations can be contrasted with an equivalent momentum equation using the free-surface elevation:

$$\frac{\partial Q}{dt}+\frac{\partial}{\partial x}\left(\beta\frac{Q^2}{A}\right)=-gA\frac{\partial \eta}{\partial x}-gAS_f \tag{3}$$

which is obtained by substitution of $\eta=H+z_b$ with z_b as the bottom elevation and $S_0=\partial z_b/\partial x$. The equation is again "conservative" by virtue of including the gradient of the free surface elevation as a source term. Comparison of eqs. (2) and (3) shows how the introduction of S_0 effects the equation form. Of particular note is that we expect $S_f=f\left(Q,A\right)$, so the latter equation will have a smooth source term as long as the solution variables themselves are smooth. In contrast, the smoothness

of the source term in eq. (2) inherently depends on the smoothness of the product AS_0. Smoothness in the source term is a mathematical necessity for the numerical solution of a partial differential equation to be well-posed (Iserles, 1996).

In general, there is an advantage to having as much of the physics as possible included on the flux-conservative side of the equation, which helps minimize difficulties in interactions associated with discretizations of the source terms (e.g., Pu et al., 2012; Vazquez-Cendon, 1999). The standard form of the conservative SVE is arguably the form provided by Cunge et al. (1980), based on a derivation of Liggett (1975):

$$\frac{\partial Q}{dt} + \frac{\partial}{\partial x}\left(\beta\frac{Q^2}{A} + gI_1\right) = gI_2 + gA\left(S_0 - S_f\right) \tag{4}$$

where I_1 and I_2 are integrated hydrostatic pressure forces across the channel

$$I_1 = \int_H (H - z)\, B\, dz \tag{5}$$

and along the channel gradients

$$I_2 = \int_H (H - z)\frac{\partial B}{\partial x} dz \tag{6}$$

with $H(x)$ as the water depth, $B(x, z)$ as the channel breadth as a function of elevation and along-stream location, and z as a coordinate direction measured from a common horizontal baseline in a direction opposite gravitational acceleration. This form is also used by others with slightly different nomenclature but the same integral terms (e.g. Hernandez-Duenas and Beljadid, 2016; Sanders, 2001; Saavedra et al., 2003). It will be convenient herein to call this the *Cunge-Liggett* form of the SVE. The key point for both these terms is that they measure the interaction between the free surface and the channel shape; e.g. I_1 could also be written as

$$I_1 = \int_{z_b}^{\eta} (\eta - z)\, B\, dz \tag{7}$$

where z_b is the channel bottom.

By comparing eq. (4) with eq. (2), we see that the novelty of Cunge-Liggett is in moving a portion of the $gA\partial H/\partial x$ from the RHS source term into the conservative flux on the LHS. Indeed, with this idea we see that eq. (2) can be used with the product rule of differentiation to generate a slightly different conservative form:

$$\frac{\partial Q}{dt} + \frac{\partial}{\partial x}\left(\beta\frac{Q^2}{A} + gAH\right) = gH\frac{\partial A}{\partial x} + gA\left(S_0 - S_f\right) \tag{8}$$

Similar to the Cunge-Liggett form, the above uses a mathematical trick to place one part of the hydrostatic pressure force within the conservative flux gradient, while retaining the remainder as a source term. Thus, we see that the Cunge-Liggett form is not canonical, nor is it a form that necessarily better represents the physics. It is merely a form that is (sometimes) convenient for splitting the gradient of the total hydrostatic pressure force into conservative flux and non-conservative source terms.

The above brings up a question: if it is good to shift a portion of the hydrostatic pressure from the source to the conservative term as in eqs. (4) and (8), then why not some or all of the gravitational potential associated with gAS_0? Underlying the Cunge-Liggett form and much (but not all) of the literature is the idea that gAS_0 is a source term that creates/destroys momentum. But this is also true of the hydrostatic pressure gradient and yet we commonly treat a portion within the convective flux. Thus, if Cunge-Liggett eq. (4) is preferred over the baseline conservative form of eq. (2) because a portion of the hydrostatic pressure is moved from the source term to the conservative flux term, then an equation that moves some (or all) of the gravitational potential from the source to the flux term should be equally valued. If this argument is accepted, then the preferred differential form for natural channels with the SVE is none of those presented above, but perhaps an equation of the general form

$$\frac{\partial Q}{dt} + \frac{\partial}{\partial x}\left\{\beta\frac{Q^2}{A} + f_1\left(A,\eta\right)\right\} = f_2\left(A,\eta\right) - gAS_f \tag{9}$$

where f_1 and f_2 are some functions (as yet unspecified) of the free-surface elevation rather than the depth. The free surface (η) can be interpreted as the uniform piezometric pressure over cross-section A, so the f_1 and f_2 functions are a generic way of splitting the piezometric pressure gradient between the source term and the conservative flux term, similar to how Cunge-Liggett handles the hydrostatic pressure gradient. Note that this proposed general approach removes the need for specifying S_0, which is important both in terms of source-term smoothness and producing "well-balanced" methods as discussed in detail in Section 3, below.

In this paper, complete derivations are presented to show that finite-volume formulations of the SVE can be generated that are consistent with the general conservative differential form of eq. (9). The new derivation is intended to bridge the gap between approaches used in high-resolution hydraulic models and those used in large-scale hydrology and urban drainage networks. The derivation provides a form of the SVE that has mathematical rigor while preserving the simplicity of the non-conservative finite-difference discretizations that are common in hydrological and urban drainage literature. Herein, we focus only on the detailed presentation of the new equation form, reserving demonstration in a numerical model to future papers.

3 Background

Origination and use of the SVE

Alexandre de Saint-Venant's equations (de Saint-Venant, 1871) were written as:

$$\frac{dA}{dt} + \frac{d\left(AU\right)}{dx} = 0 \tag{10}$$

$$-\frac{d\eta}{dx} = \frac{1}{g}\frac{dU}{dt} + \frac{U}{g}\frac{dU}{dx} + \frac{\ell_p}{A}\frac{F}{\rho g} \tag{11}$$

where U is the velocity, ℓ_p is the wetted perimeter, and F is the frictional force per unit bottom area along the channel, and other terms are as previously noted. We have taken the liberty of replacing Saint-Venant's notation of w, ζ, χ, s with the more modern nomenclature of A, η, ℓ_p, x, but otherwise have retained the original form. The momentum equation of de Saint-Venant, eq. (11), is identical to eq. (1) if we use $Q = AU$, $S_f = \ell_p F/\left(g\rho A\right)$, integrate over a cross-section with the β coefficient, apply

some calculus with the continuity equation, and define $\eta \equiv H + z_b$ along with $S_0 = -\partial z_b / \partial x$. From a practical perspective, the only thing that a hydrologist really needs to change from the original equation set is to replace the zero on the right-hand-side of eq. (10) with a source term representing the inflow/outflow per unit length from/into the catchment and groundwater. However, from a numerical modeling perspective, eq. (11) is fundamentally non-conservative and suitable only for discretization in finite-difference forms. Although the full equation set is sometimes called the SVE, for convenience in exposition we will use SVE as a shorthand for the momentum equation alone.

The SVE are ubiquitous in the literature for a wide range of work and have a foundational role in flow routing schemes in hydrological models and channel network models for urban drainage. However, there is an interesting gap between the equation forms used in large-scale systems and those used in shorter single-reach studies or modeling hydraulic features. For computational simplicity, large-scale network flow models often use a reduced set of equations, such as Muskingum, kinematic wave, or the local inertia form (e.g. Wang et al., 2006; David et al., 2011, 2013; Getirana et al., 2017). Herein, we will follow the arguments of Hodges (2013) that we should be using the full SVE and the reduced-physics models are principally a stop-gap measure as we wrestle with obtaining satisfactory SVE solution methods. As computational power has increased large-scale models have been moving towards the full SVE, but typically in a non-conservative form (e.g. Paiva et al., 2013; Liu and Hodges, 2014). For urban drainage networks, the US EPA Storm Water Management Model (SWMM) and variants built on this public domain model use a non-conservative finite-difference form of the SVE. This model is widely applied (e.g. Gulbaz and Kazezyilmaz-Alhan, 2013; Hsu et al., 2000; Krebs et al., 2013), however deficiencies in conservation are a recognized problem (Rossman, 2017) and the SVE solver is the critical computational expense in the modeling system (Burger et al., 2014). Engineering river hydraulics problems are often solved using the U.S. Army Corps of Engineers HEC-RAS software, which has free model executables with a proprietary (closed-source) code base. HEC-RAS uses a non-conservative finite-difference form of the SVE based on methods pioneered in the 1970s (Brunner, 2010). In contrast, more recent research models of the SVE at short river-reach scales have typically used the equations presented as hyperbolic conservation laws that ensure both conservation and well-behaved solutions for subcritical, supercritical, and transcritical flows (e.g. Guinot, 2009; Ivanova et al., 2017; Papanicolaou et al., 2004; Sanders et al., 2003).

There is also a vast gulf between the spatial discretization of SVE for large systems and smaller system studies in the hydraulics and applied mathematics literature (although the gap is getting narrower). For example in 2003 the SVE were solved at 1 to 4 km spacing for 156 km of river (Saavedra et al., 2003). Seven years later we find 4 km cross-section spacing for 5×10^3 km of river (Pramanik et al., 2010). By 2014 the state-of-the-art was 100 m spacing for 15×10^3 km of river (Liu and Hodges, 2014). In contrast, hydraulic studies have typically focused on 1 to 10 m spacing for 1 to 2 km test cases (e.g. Gottardi and Venutelli, 2003; Kesserwani et al., 2009; Sart et al., 2010; Venutelli, 2006). Between these extremes, single-reach river models with natural geometry are typically modeled over river lengths less than 20 km with grid cells on the order of 10 m to more than 100 m (Sanders et al., 2003; Catella et al., 2008; Castellarin et al., 2009; Lai and Khan, 2012).

Preissmann *v.* Godunov

Computational modeling of the SVE is arguably a long-running contest between the differential, finite-difference governing equations pioneered Preissmann (1961) and the integral, finite-volume formulations derived from Godunov (1959). Clearly, this is a simplification as there are wide-ranging contributions across both numerical methods and implementation schemes – but the literature is simply too broad to discuss all developments in anything less than a book. Nevertheless, using a dialectic of Preissmann *v.* Godunov is a useful way of thinking about the major developments as context of the equations derived herein. Preissmann developed effective finite-difference methods applied to the non-conservative form of the equations and is the first basis for comparison of succeeding finite-difference models. The introduction of Roe's approximate Riemann solver (Roe, 1981) and analyses of Harten et al. (1983) made Godunov-like methods tractable and set off a multi-decadal development of finite-volume methods. The literature with these two methods is vast, but a reasonable cross-section is provided in Table 1. Beyond these two major families, a variety of other schemes have been applied including finite-element methods (e.g., Szymkiewicz, 1991; Venutelli, 2003), finite-volume methods that do not use the Godunov approach (e.g. Audusse et al., 2004, 2016; Catella et al., 2008; Katsaounis et al., 2004; Mohamed, 2014; Vazquez-Cendon, 1999; Xing and Shu, 2011; Ying et al., 2004), and finite-difference methods that do not apply the Preissmann scheme (e.g., Abbott and Ionescu, 1967; Arico and Tucciarelli, 2007; Buntina and Ostapenko, 2008; Schippa and Pavan, 2008; Tucciarelli, 2003; Wang et al., 2000). Discontinuous Galerkin (DG) methods have recently been introduced, which can be thought of as a higher-order Godunov method (e.g., Kesserwani et al., 2008, 2009; Lai and Khan, 2012; Xing, 2014; Xing and Zhang, 2013).

It is clear from the above that there is no consensus on the best method for solving the SVE. For high-resolution modeling that correctly preserves shocks and transcritical flows, it can be reasonably argued that finite-volume and DG schemes are more successful than finite-difference schemes. Beyond that broad observation, the question of whether a finite-volume method with Godunov-like approach is better than non-Godunov approach does not have a clear answer either in terms of accuracy or computational run times. However, in terms of large-scale systems the Preissmann scheme and finite-difference methods presently reign supreme with the ability to solve more than 15×10^3 km of river on a desktop computer (Liu and Hodges, 2014). Nevertheless, we can see that a conservative finite-volume approach for large-scale systems would be preferred as the basis for problems in Continental River Dynamics (Hodges, 2013) as well as for the challenges of urban drainage modeling for the mega-cities that are growing across the earth. Being able to control numerical dissipation of momentum and ensure conservative fluxes will be increasingly important as advancing computing power pushes down the practical model grid scales.

The "well-balanced" problem and S_0

That finite-volume solutions are not commonly used in large-scale hydrologic and urban drainage models is a testament to their complexity. The difficulties associated with finite-volume solutions using the Cunge-Liggett conservative form of the SVE have engendered a broad literature on "well-balanced" schemes deriving from the study of Greenberg and Leroux (1996). A principle feature of a well-balanced scheme is that it provides exactly steady solutions for exactly steady flows. The most trivial requirement, which is often not met, is that a flat free surface should result in exactly zero velocities. This problem is

Table 1. Two decades of Preissman v. Godunov

Preissman	Godunov
Canelon (2009)	Bollermann et al. (2013)
Casas et al. (2010)	Delis and Skeels (1998)
Castellarin et al. (2009)	Delis et al. (2000b)
Chau and Lee (1991)	Delis et al. (2000a)
Chen et al. (2005)	Ferreira et al. (2012)
Gasiorowski (2013)	Gottardi and Venutelli (2003)
Islam et al. (2008)	Goutal and Maurel (2002)
Leandro and Martins (2016)	Greenberg and Leroux (1996)
Liu and Hodges (2014)	Guinot (2009)
Lyn and Altinakar (2002)	Ivanova et al. (2017)
Paiva et al. (2011, 2013)	Kesserwani et al. (2010)
Paz et al. (2010)	Kurganov and Petrova (2007)
Rosatti et al. (2011)	Li and Chen (2006)
Saavedra et al. (2003)	Liang and Marche (2009)
Sart et al. (2010)	Monthe et al. (1999)
Saleh et al. (2013)	Pu et al. (2012)
Sen and Garg (2002)	Sanders (2001)
Venutelli (2002)	Sanders et al. (2003)
Wu et al. (2004)	Venutelli (2006)
Zeng and Beck (2003)	Wu and Wang (2007)
Zhu et al. (2011)	Ying and Wang (2008)

readily illustrated by considering eq. (4) with $Q = 0$, where the free surface should be exactly flat and $S_f = 0$. Achieving the simple result of $Q = 0$ for a flat free surface with the Cunge-Liggett form requires

$$\frac{\partial I_1}{\partial x} = I_2 + AS_0 \iff H + z_b = \text{constant} \tag{12}$$

which implies the Cunge-Ligget form is only well-balanced if the geometry meets the following identity at every possible water surface level:

$$\frac{\partial}{\partial x} \int_{z_b(x)}^{z_R} (z_R - z)\, B\, dz - \int_{z_b(x)}^{z_R} (z_R - z)\, \frac{\partial B}{\partial x}\, dz = AS_0 \quad : \quad z_b < z_R \leq \eta_{max} \tag{13}$$

where η_{max} is the maximum water surface elevation, $z_b(x)$ is the local channel bottom elevation, and z_R encompasses all possible water surface elevations. Clearly, designing a numerical scheme that *exactly* preserves this relationship for non-uniform

channels is a challenge, as evidenced by the breadth and complexities of studies focused on this issue (e.g., Audusse et al., 2004; Bollermann et al., 2013; Bouchut and Morales de Luna, 2010; Castro Diaz et al., 2007; Crnković et al., 2009; Kesserwani et al., 2010; Kurganov and Petrova, 2007; Li et al., 2017; Liang and Marche, 2009; Perthame and Simeoni, 2001; Xing, 2014). Failure to satisfy the well-balanced criteria results in models that generate spurious velocities; i.e., a mismatch in eq. (13) indicates that the numerics provide momentum sources/sinks that are functions of channel shape and discretization rather than flow physics. An interesting approach to this problem was developed by Schippa and Pavan (2008) where eq. (12) is used to replace $I_2 + AS_0$ in the source term with $\partial I_1/\partial x$ evaluated for a horizontal surface. Their approach ensures that *any* discretization will be well-balanced for a zero-velocity flow.

The work of Schippa and Pavan (2008) and a review of other works on well-balanced schemes provides us a key insight: the principal challenge for obtaining a well-balanced method is the channel bottom slope, S_0, which is often sharply varying or even discontinuous in a natural system. Furthermore, as a geometrical property, S_0 should be independent of the cross-sectional flow area (A), and yet is forced to be discretely related through eq. (12). If we take this idea a step further, we can argue that the fundamental problem with the Cunge-Liggett form is that the physical forces that alter momentum (gravitational potential and hydrostatic pressure) are arbitrarily separated so that one is wholly within the source term and the other has an *ad hoc* split between conservative flux and source terms. Thus, we return to the idea put forward in the Introduction that we should consider the free surface elevation (piezometric pressure) instead of the water depth (hydrostatic pressure) as our primary forcing gradient.

In the next section, we shall see how the ideas of shifting portions of the total piezometric pressure from source to flux can be used to develop a rigorous finite-volume form of the SVE that is simpler those based on the Cunge-Liggett form.

4 Finite-volume SVE with minimal approximations

Continuity

Although we are focused on the momentum equation, for completeness we will start with continuity. The general arrangement of the control volume for an irregular channel and the vectors used in the following discussion are illustrated in Fig. 1. Applying only the incompressibility approximation for a uniform density fluid, the volume-integrated continuity equation is

$$\frac{\partial V}{\partial t} + \oint_S u_k n_k \, dA = S_V \tag{14}$$

where the Einstein summation convention is applied on repeated subscripts, u_k is a vector velocity, and n_k is a unit normal vector defined as positive pointing outward from a control volume V, and S_V is a volume source ($S_V < 0$ for a sink).

A semi-discrete finite volume representation of continuity can be directly written as

$$\frac{\partial V_e}{\partial t} = Q_u - Q_d + q_e L_e \tag{15}$$

where Q, and L represent the flow rate and element length, and subscripts e, u, and d denote characteristic values for the control volume element, nominal upstream face, and nominal downstream face, respectively. Here we use the "nominal" flow direction

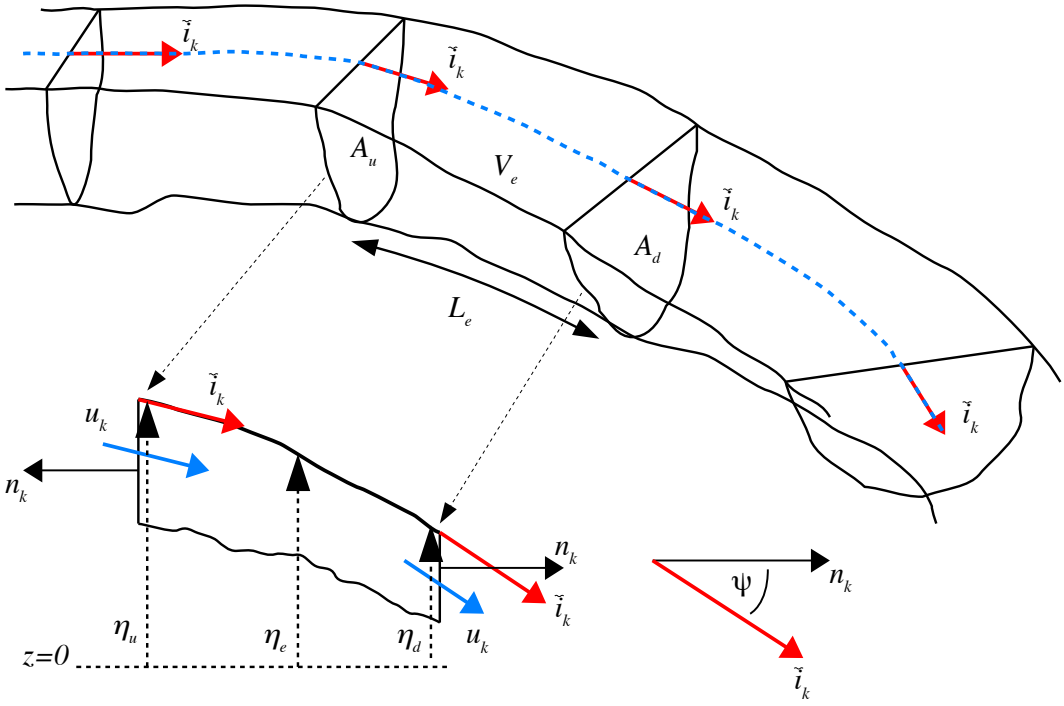

Figure 1. General arrangement of control volume element (V_e) and its neighbors for irregular channel. Unit normal vectors n_k are always perpendicular to cross-sectional areas (A_u, A_d) and pointing outward from control volume. The element length (L_e) is measured along the channel. Unit vectors $\hat{i}_k$ are coincident with the free surface slope in the streamwise direction and can be defined as local continuous functions. The velocity vector u_k is approximated as parallel to $\hat{i}_k$. The angle measured from n_k to $\hat{i}_k$ is ψ. The free surface elevations η_u, η_e, and η_d, are cross-section uniform elevations at the upstream face, for the element center, and the downstream face, respectively. Note that volume is V throughout the derivations with u and U used for continuous and spatially-averaged velocities, respectively.

as the global downhill direction of the channel that is assigned at the network level. The average lateral inflow per unit length is q_e, and a flow $Q > 0$ is from the upstream to downstream direction. Reversals of flow from the nominal flow direction are handled with $Q < 0$.

Momentum

The control-volume form of the Navier-Stokes momentum equation in a direction defined by unit vector $\hat{i}$ in a Cartesian frame is

$$\frac{\partial}{\partial t}\int_V u_{\hat{i}}\,dV + \oint_S u_{\hat{i}} u_k n_k\,dA + \frac{1}{\rho}\oint_S p\hat{i}_k n_k\,dA = \oint_S \nu\frac{\partial u_j}{\partial x_k}\hat{i}_j n_k\,dA + \int_V g_{\hat{i}}\,dV \tag{16}$$

where $u_{\hat{i}}$ is a velocity vector component in the $\hat{i}$ direction, u_k are velocity components along the Cartesian axes, the gravity vector is $g_{\hat{i}}$ in the $\hat{i}$ direction, ν is the kinematic viscosity, and p represents the thermodynamic pressure. Note that this formulation can be related to any arbitrary Cartesian axes. In many common derivations, $\hat{i}$ is approximated as coincident with an x axis that is a *horizontal* vector in the streamwise direction. In the following, we will show that this approximation is not required. Instead, we treat this as a simplification that can be applied to the final equation form.

Advection terms

The $\hat{i}$ direction for momentum, eq. (16), is a vector associated with the $u_{\hat{i}}$ velocity component, which is not necessarily coincident with the normal vector n_k at a surface of a finite volume (in contrast to the case where $\hat{i}$ is taken as horizontal). For a gradually-varying open-channel flow we can take the $\hat{i}$ vector as the nominal downstream direction along the channel centerline described by a vector *that lies along the free surface*, as illustrated in Fig. 1. Thus, this vector is local (as opposed to being forced into coincidence with a Cartesian axis) and changes along the channel with the slope of the free surface. It follows that the discrete control volume formulation is globally exact as $V_e \to 0$. In contrast, a derivation that takes $\hat{i}$ as a vector in the horizontal direction has a momentum conservation error proportional to $\cos\psi$, where ψ is an angle between the horizontal vector and the free surface; such an error does not vanish as $V_e \to 0$ unless the free surface is flat across the length of the element. This idea helps illustrate one of the subtle advantages of the Godunov approach in which the channel is imagined as having a piecewise flat free surface: $\cos\psi = 1$ is then an identity within the approximation of the physics, rather than as an approximation within the mathematics.

The upstream element face is required to be vertical and normal to the smooth channel centerline in a horizontal plane, as illustrated in Fig. 1. The free surface at the centerline has an angle of $\psi(x)$ to the horizontal so that the discrete nonlinear momentum term in the $\hat{i}$ direction across the upstream face is formally

$$\int_{A_u} u_{\hat{i}} u_k n_k dA = \beta Q_u U_u \cos\psi_u \tag{17}$$

where u subscripts indicate the upstream face (rather than vector components), $\hat{i}$ is defined normal to the surface, U is the average velocity normal to the face (which implies $Q = UA$), and β is the momentum coefficient for the streamwise velocity, defined as

$$\beta \equiv \frac{1}{A\left[U(x)\right]^2}\int_A \left[u(x,y,z)\right]^2\,dA \tag{18}$$

Note that the convective term of eq. (17) does not contain any approximations.

It is convenient to let the M_e represent the integrated sources (+) and sinks (−) of momentum per unit mass in the finite-volume element associated with the $q_e L_e$ lateral fluxes of eq. (15). Furthermore, *if the channel is straight* so that $\hat{i}$ at the upstream face is parallel to $\hat{i}$ at the downstream face, it follows that an exact finite-volume integration is

$$\oint_S u_{\hat{i}} u_k n_k \, dA = -\mathrm{sgn}(U_u)\, \beta_u Q_u U_u \cos\psi_u + \mathrm{sgn}(U_d)\, \beta_d Q_d U_d \cos\psi_d - M_e \tag{19}$$

where $\mathrm{sgn}(U)$ is a sign function returning $+1$ for $U > 1$, -1 for $U < 1$, and 0 for $U = 0$. For the more general case where the channel is curved between the upstream and downstream faces (as in Fig. 1), the above integration becomes an approximation – i.e. the effects of cross-channel gradients on the nonlinear advective term are neglected in the discrete form. For present purposes, the use of a $\hat{i}$ direction that follows the curving channel implies that pressure is perfectly redirecting momentum through the bend. This redirection is not precisely correct as secondary circulation in bends affects bed shear, velocity distribution, and frictional losses (Blanckaert and Graf, 2004). Arguably, losses associated with flow-redirection in channel bends should be built into the frictional term in any model. Unfortunately, this remains a relatively poorly-studied area at the interface of hydrology and hydraulics. The curvature effects on the equations can be written as perturbation terms that relate the channel width to the radius of curvature (Hodges and Imberger, 2001; Hodges and Liu, 2014), but these ideas have yet to be exploited in developing curvature effects in SVE numerical models.

Pressure decomposition

For the pressure term in eq. (16) we follow the traditional approach for incompressible flows of defining a modified pressure ($\tilde{P}$) that includes the gravity term, which requires $\tilde{P} = p + \rho g z$. More formally we define

$$\frac{1}{\rho}\oint_S \tilde{P}\hat{i}_k n_k \, dA \equiv \frac{1}{\rho}\oint_S p\hat{i}_k n_k \, dA - \int_V g_{\hat{i}} \, dV \tag{20}$$

The surface integral for the modified pressure decomposes into integrations over the upstream cross-section (A_u), the downstream cross-section (A_d) the channel bottom (A_B), and the free surface (A_η) as:

$$\frac{1}{\rho}\oint_S \tilde{P}\hat{i}_k n_k \, dA = \frac{1}{\rho}\left\{ \int_{A_u} \tilde{P}\hat{i}_k n_k \, dA + \int_{A_d} \tilde{P}\hat{i}_k n_k \, dA + \int_{A_B} \tilde{P}\hat{i}_k n_k \, dA + \int_{A_\eta} \tilde{P}\hat{i}_k n_k \, dA \right\} \tag{21}$$

The above is an exact pressure term without imagining the geometry to be rectilinear or that the free surface has any simplified shape. The only geometric requirement of the volume is that faces A_u and A_d must be vertical planes that cut across the channel, which is necessary for consistency with the convective term. The first simplification we can introduce is to approximate the free surface as uniform at any cross section. The slope of the free surface is then everywhere coincident with the $\hat{i}(x)$ vector, which is aligned with the free surface at the channel centerline. With the free surface aligned with $\hat{i}(x)$, the modified pressure is everywhere normal to the free surface and cannot contribute to the streamwise momentum (which we have defined as parallel to $\hat{i}(x)$ in deriving the advection terms, above). It follows that $\tilde{P}\hat{i}_k n_k$ is identically zero at the free surface and the last term in eq. (21) vanishes.

Piezometric and non-hydrostatic pressure

It will be convenient to introduce a decomposition of the modified pressure ($\tilde{P}$) into a piezometric pressure (P) and non-hydrostatic pressure ($\breve{P}$), where only the latter is non-uniform over a cross-section.. The non-hydrostatic pressure is defined by the difference between the modified pressure and the piezometric pressure:

$$\breve{P}(x,y,z) \equiv \tilde{P}(x,y,z) - P(x) \tag{22}$$

The piezometric pressure is formally the sum of the hydrostatic pressure and the gravitational potential at any point z for $z_b \le z \le \eta$, which provides $P(x,y,z) \equiv \rho g\left[\eta(x,y) - z\right] + \rho g z = \rho g \eta(x,y)$. For the SVE, the free surface elevation can be considered uniform over the channel breadth (i.e., neglecting cross-channel tilt in channel bends). It follows that the piezometric pressure is

$$P(x) = \rho g \eta(x) \tag{23}$$

which is uniform over a vertical cross section. The non-hydrostatic pressure was neglected by Alexandre de Saint-Venant and arguably should be neglected in any 1D momentum equation bearing his name. However, for completeness we will retain the non-hydrostatic pressure terms in the derivation below, but it will be neglected in discrete forms of the piezometric pressure terms in Section 5.

Pressure on flow faces

To further simplify the first two pressure terms in eq. (21), we define $\psi(x)$ as the angle between a horizontal line and the free surface, $\eta(x)$, measured clockwise positive from the horizontal line pointing downstream. Thus, the $\hat{i}$ vector is generally at an angle $\pm\psi(x)$ and pointing in the nominal downstream direction, as shown in Fig. 1. At the upstream cross-section the pressure force without approximations is

$$\int_{A_u} \tilde{P}\,\hat{i}_k n_k\,dA = -\cos\psi_u \int_{A_u} \tilde{P}(x,y,z)\,dA \tag{24}$$

where subscript u indicates values at the upstream cross section. Similarly, the downstream cross-section provides

$$\int_{A_d} \tilde{P}\,\hat{i}_k n_k\,dA = +\cos\psi_d \int_{A_d} \tilde{P}(x,y,z)\,dA \tag{25}$$

where subscript d indicates values at the downstream cross section. Note that in the above and in the following derivations, the ubiquitous $1/\rho$ coefficient of all pressure terms will be omitted for clarity. Introducing the piezometric and non-hydrostatic pressure split of eq. (22) provides:

$$\int_{A_u} \tilde{P}\,\hat{i}_k n_k\,dA = -P_u A_u \cos\psi_u - \cos\psi_u \int_{A_u} \breve{P}(x,y,z)\,dA \tag{26}$$

$$\int_{A_d} \tilde{P}\hat{i}_k n_k \, dA = +P_d A_d \cos\psi_d + \cos\psi_d \int_{A_d} \breve{P}(x,y,z)\, dA \tag{27}$$

Note that using the piezometric pressure instead of the hydrostatic pressure ensures that the only term requiring a formal integration at the upstream and downstream surfaces is the non-hydrostatic pressure.

Pressure on bottom

The third pressure term in eq. (21) is more challenging than the pressure on the flow faces. To arrive at a simpler formulation, we note the channel bottom has some local angle $\hat{\theta}(x,y)$ to the horizontal (i.e., the local bottom slope angle), which is measured clockwise from a downstream-pointing horizontal line to the bottom as illustrated in Fig. 2. Here we need to assume that cross-channel variations can be represented with a characteristic slope, $\theta(x)$, which adequately represents the true variability of $\hat{\theta}(x,y)$ across the channel at location x. The modified pressure ($\tilde{P}$) at the bottom is, by definition, normal to the bottom, so where $\theta(x) = \psi(x)$ the bottom is exactly parallel with the free surface and the pressure at the bottom is exactly normal to $\hat{i}$ and thus normal to the streamwise flow. It follows that under this restricted condition the integral of $P\hat{i}_k n_k$ over A_B is identically zero and the third pressure term in eq. (21) vanishes – that is, gradients in pressure that are normal to the streamwise direction cannot alter momentum. However, for the more general case when the bottom and the free surface are not precisely parallel, $\tilde{P}$ at the bottom can be decomposed into a component acting normal to the free surface and a component parallel to the free surface (i.e., a modified bottom pressure contribution acting along the $\hat{i}$ flow direction), as shown in Fig. 2. The effect of the bottom topography acting on the fluid can be represented as

$$\int_{A_B} \tilde{P}\hat{i}_k n_k \, dA \approx -\int_{A_B} \left|\tilde{P}(x,y,z)\right| \sin\left[\theta(x) - \psi(x)\right] dA \tag{28}$$

where the sign of the term is selected for consistency with the $\hat{i}$ nominal downstream direction and the definitions of θ and ψ to provide for the correct sense in either diverging ($\theta > \psi$) or converging ($\theta < \psi$) conditions. The condition $\theta > \psi$ implies that the fluid pressure at the bottom (normal to θ) will have a component in the upstream direction when decomposed into vectors normal and tangent to the ψ of the free surface, which means the force of the bottom on the fluid is acting downstream, with a normal vector (n_k) that points outward from the element (e.g., upstream). Note that this approach allows consideration of adverse free surface gradients ($\psi < 0$) and adverse slope angles ($\theta < 0$) without any special treatment.

To develop a simpler implementation of the bottom pressure term, we need an approximation for the contribution of the vector component of pressure along the bottom that is aligned with the $\hat{i}$ direction of the free surface. That is, we can neglect the bottom pressure contribution that is perpendicular to $\hat{i}$ since it cannot contribute to streamwise momentum. We introduce a conceptual model with the channel bottom imagined as $m = 1...N$ stairsteps where the treads are locally parallel to the free surface and the risers are normal to the free surface, as illustrated in Figs. 3 through 5.

Clearly, as $N \to \infty$ we will recover a continuous approximation so there is no need to actually consider the discrete stair steps in a solution method – the stair-steps are merely to illustrate what is otherwise a mathematical abstraction in vector

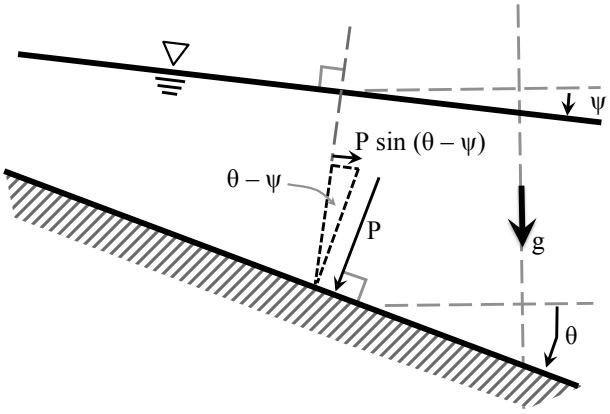

Figure 2. Pressure decomposition to obtain streamwise contribution.

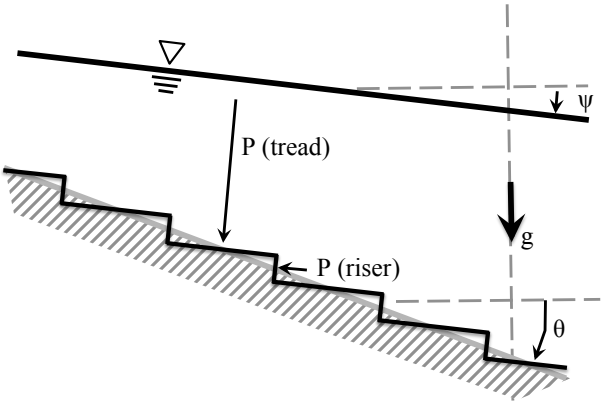

Figure 3. Stair-step approximation for pressure along bottom where tread is parallel to the free surface and riser is perpendicular for linear slopes of both bottom and free surface.

calculus. We can imagine the stair-step risers as thin planar strips across the entire wetted perimeter that provide a discrete representation of irregular channel cross-section structure, as illustrated in Fig. 6. The only approximations needed for this conceptual model are: (1) the free surface at longitudinal position x is uniform over the cross-section and aligned with $\hat{i}(x)$, and (2) the channel topography at longitudinal position x has a characteristic slope angle $\theta(x)$ that is uniform over the cross section. Since the stair-step treads are (by definition), normal to the modified pressure above, it follows that the only pressure contributions to the momentum in the streamwise $\hat{i}$ direction are on the risers, with individual areas $A_{R(m)}$ for $m = 1...N$ stairsteps. Because the pressure contribution for increasing cross-sectional area (i.e., steps down as in Fig. 3) will be opposite of the pressure contribution for decreasing cross-sectional are (i.e., steps upward, see downstream section of Fig. 5), it is convenient to introduce a function $\gamma_{(m)} = \pm 1$ to account for the change of sign needed for the direction of the pressure force.

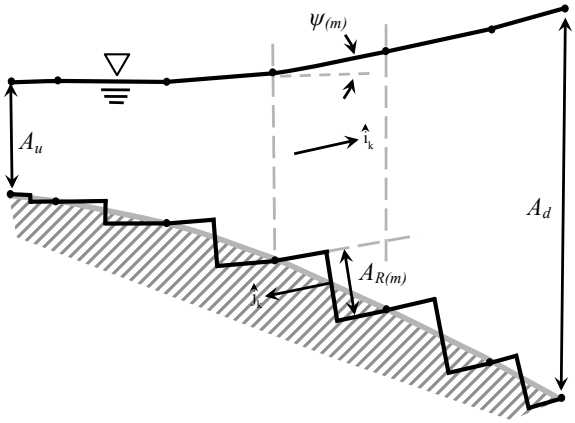

Figure 4. Conceptual model of piecewise linear approximation of nonlinear free surface and stair-step approximation of nonlinear bottom with cross-sectional area monotonically increasing. Pressure on the discrete riser area $A_{R(m)}$ is locally aligned with free surface slope directly above. The vertical scale and thus the tilt of $A_{R(m)}$ are exaggerated for illustrative purposes.

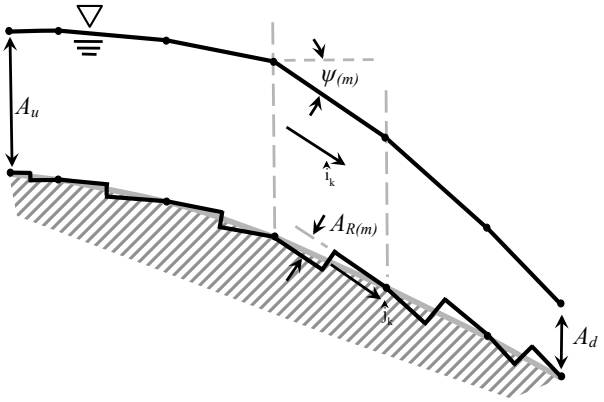

Figure 5. Conceptual model of piecewise linear approximation of nonlinear free surface and stair-step approximation of nonlinear bottom with cross-sectional area increasing from A_u to the center and then decreasing from the center to A_d. Pressure on the discrete riser area $A_{R(m)}$ is locally aligned with free surface slope directly above. The vertical scale and thus the tilt of $A_{R(m)}$ are exaggerated for illustrative purposes. Note that the bottom slope is identical to Fig. 4 but the stair steps are different due to the alteration of the free surface.

We can formally define $\gamma_{(m)} \equiv \hat{i}_k \hat{j}_k$ at step m where $\hat{j}_k$ is the normal unit vector (pointing outwards) from the $A_{R(m)}$ riser, as

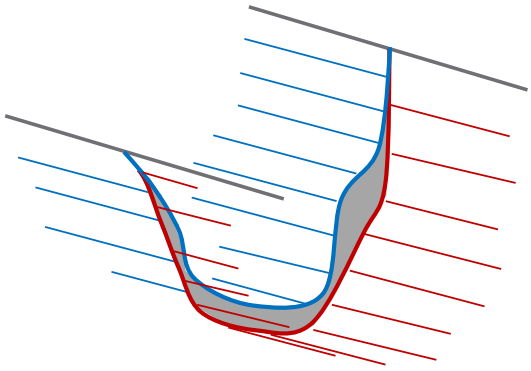

Figure 6. Three-dimensional conceptual model of stair-step riser (gray) as a 2D plane area of $A_{R(m)}$ separating two tread areas (blue, red).

shown in Figs. 4 and 5. It follows that

$$\int_{A_B} \tilde{P}\hat{i}_k n_k \, dA \approx -\sum_{m=1}^{N} \gamma_{(m)} \int_{A_{R(m)}} \tilde{P}(x,y,z)\, dA \tag{29}$$

The above summation can be written as an integral over the length L of the finite-volume element as $N \to \infty$.

$$\int_{A_B} \tilde{P}\hat{i}_k n_k \, dA = -\int_{L} \gamma(x) \int_{A_R(x)} \tilde{P}(x,y,z)\, dA\, dx \tag{30}$$

where $\gamma(x) = \hat{i}_k \hat{j}_k$ is the continuous counterpart to the discrete $\gamma_{(m)}$. Note that this conceptual model is valid even for non-monotonic behavior of the riser area (e.g., Fig. 5) as long as the $A_{R(m)}$ are continuous and smooth as $N \to \infty$ and the approximation of $\theta(x)$ as the slope of the channel cross-section is reasonable for all $\hat{\theta}(x,y)$ across the channel. However as discussed in Section 5, below, extremes of non-monotonic behavior can make it difficult to create a consistent discrete equation for the bottom pressure.

For further simplification, it is convenient to introduce the piezometric/non-hydrostatic splitting of eq. (22) where, by definition, the piezometric pressure is is uniform over a vertical cross section (e.g., a stair-step riser). Let $P_{(m)}$ represent the piezometric pressure at the m stair-step riser with area $A_{R(m)}$ so that over a control volume for steps $m = 1...N$. It follows that

$$\begin{aligned} \sum_{m=1}^{N} \int_{A_{R(m)}} P_{(m)}\, dA &= \sum_{m=1}^{N} P_{(m)} \int_{A_{R(m)}} dA \\ &= \int_{L} P(x) A_R(x)\, dx \end{aligned} \tag{31}$$

where the continuous $A_R(x)$ represents the effective bottom area contributing to the piezometric pressure force in the streamwise $\hat{i}(x)$ direction. Applying this continuous $A_R(x)$ form and the hydrostatic/nonhydrostatic splitting to eq. (30), we obtain

$$\int_{A_B} \tilde{P}\hat{i}_k n_k \, dA = -\int_L \gamma(x) P(x) A_R(x) \, dx - \int_L \gamma(x) \int_{A_R} \breve{P}(x,y,z) \, dA \, dx \tag{32}$$

The stair-step conceptual model and A_R allow us to consider the pressure effects along the $\hat{i}$ direction due to the changing cross-sectional area of the channel without introducing the separate force terms I_1 and I_2 of the Cunge-Liggett form of the SVE. An interesting part of this model is that $A_R(x)$ over a control volume is a function of *both* the local bottom topography and the local free surface slope. That is, if we imagine either Fig. 3 or 4 with a flat free surface it should be immediately obvious that the $A_{R(m)}$ riser areas would be different. Thus, A_R is a dynamic representation of the interaction between the free-surface gradient and bottom topography that controls the effective along-stream pressure gradient of converging or diverging flow areas. However, we do not want to directly compute $\int P A_R \, dx$ over a control volume – it seems likely that direct discretization of subgrid topography could easily result in creating unbalanced momentum source terms. In effect, computing $\int P A_R \, dx$ has the same complexity as computing the I_1 or I_2 terms of the Cunge-Liggett form. Thus, it is useful to consider limiting approximations that can be developed from examining the geometry of Figs. 3 and 4. In the simplest case where both the free surface and bottom have linear slopes (Fig. 3), geometry requires that

$$A_d \cos\psi - A_u \cos\psi = \sum_{m=1}^{N} A_{R(m)} \tag{33}$$

where $A_d \cos\psi$ represents the cross-sectional area normal to the free surface at the downstream cross section and there is only one value of ψ across the control volume. Note that the above is an identity for any discrete N stairsteps for the linear case. The geometry is somewhat more complex for the nonlinear system of Fig. 4, but the m stair step with free surface angle $\psi_{(m)}$ must satisfy a similar geometric identity

$$A_{(m-1/2)} \cos\psi_{(m)} - A_{(m+1/2)} \cos\psi_{(m)} = A_{R(m)} \tag{34}$$

where $A_{(m\pm1/2)} \cos\psi_{(m)}$ are the areas normal to the free surface on the upstream and downstream edges of the m piecewise linear stair step. For the nonlinear free surface and/or topography over adjacent linear stair-steps there is a discontinuity of the treads for adjacent steps as $\cos\psi_{(m-1)} \neq \cos\psi_{(m)}$, so the discrete summation of the stair step areas over a control volume provides an approximation rather than an identity:

$$A_d \cos\psi_d - A_u \cos\psi_u \approx \sum_{m=1}^{N} A_{R(m)} \tag{35}$$

However, in the limit as $N \to \infty$ we have a single value of $\cos\psi$ at any point along a smooth free surface so that the continuous form provides an identity:

$$A_d \cos\psi_d - A_u \cos\psi_u = \int_L A_R(x) \, dx \tag{36}$$

To generalize the above for $A_d < A_u$, we can use the $\gamma(x) = \pm 1$ that was introduced for the pressure direction in eq. (30). Values of $\gamma(x) = +1$ indicates the cross-section area is increasing across location x in the streamwise direction (as in Figs. 3 and 4), whereas $\gamma(x) = -1$ indicates the cross-sectional area is decreasing (as in the latter portion of Fig. 5). It follows that

$$A_d \cos\psi_d - A_u \cos\psi_u = \int_L \gamma(x) A_R(x)\, dx \tag{37}$$

is an identity that should be satisfied for a control volume with any continuous, smooth bottom topography and free surface.

To handle $A_R(x)$ in the pressure term of eq. (32), we introduce a quadrature function $\lambda(x)$, defined as

$$\lambda(x) \equiv \frac{\gamma(x) A_R(x)}{A_d \cos\psi_d - A_u \cos\psi_u} \tag{38}$$

Note that eq. (37) implies the identity:

$$\int_L \lambda(x)\, dx = 1 \tag{39}$$

Using the above in the first term on the RHS of eq. (32), we obtain

$$\int_L \gamma(x)\, P(x)\, A_R(x)\, dx = (A_d \cos\psi_d - A_u \cos\psi_u) \int_L P(x)\, \lambda(x)\, dx \tag{40}$$

Thus, the introduction of λ allows us to extract a multiplier from the control volume integral of the bottom pressure. As a result, $\lambda(x)$ is merely a distribution, or "weighting" function for integration of $P(x)$. The full bottom pressure term, eq. (32), can be written as

$$\int_{A_B} \tilde{P}\, \hat{i}_k n_k\, dA = -(A_d \cos\psi_d - A_u \cos\psi_u) \int_L P(x)\lambda(x)\, dx - \int_L \gamma(x) \int_{A_R} \breve{P}(x,y,z)\, dA\, dx \tag{41}$$

Note that λ weighting cannot be readily applied the non-hydrostatic term because the non-hydrostatic pressure on the bottom has spatial distributions in both the vertical and across a channel that cannot be assumed negligible; hence we cannot pass $\breve{P}$ through the A_R integration as was done in eq. (31) for P.

We can think of $\lambda(x)$ as a weighting function of the conceptual stair-step riser areas over the control-volume length, which controls where the piezometric pressure gradients have their greatest effect. For example, in Fig. 3 the stair-step risers are uniformly distributed such that we can use $\lambda(x) = L^{-1}$, which meets the identity requirement of eq. (39). In contrast, Fig. 4 implies $\lambda(x)$ is perhaps a quadratic function. Figure 5 presents a challenge as $\lambda(x)$ should reverse in sign between the upstream and downstream faces. A key point in this new finite-volume derivation is the selection of λ functions provides a more general discrete control over the representation of the free surface and bottom topography within a control volume. This can be contrasted to the Godunov approach that approximates a control volume as piecewise uniform for both the bottom elevation and free surface elevation over a control volume (see Section 3). Several discrete approaches to approximation of $\lambda(x)$ will be examined in Section 5, although the full consequences and utility of the λ approach will require more extensive investigation for both theoretical limitations and practical discretization schemes.

Combining pressure terms

In summary, the pressure terms of eq. (21) can be written using eqs. (26), (27) and (41), resulting in:

$$\frac{1}{\rho}\oint_S \tilde{P}\hat{i}_k n_k\,dA = -\frac{1}{\rho}A_u P_u\cos\psi_u + \frac{1}{\rho}A_d P_d\cos\psi_d - \frac{1}{\rho}\left(A_d\cos\psi_d - A_u\cos\psi_u\right)\int_L P(x)\lambda(x)\,dx$$
$$-\frac{\cos\psi_u}{\rho}\int_{A_u}\breve{P}(x,y,z)\,dA + \frac{\cos\psi_d}{\rho}\int_{A_d}\breve{P}(x,y,z)\,dA - \frac{1}{\rho}\int_L\gamma(x)\int_{A_R}\breve{P}(x,y,z)\,dA\,dx \tag{42}$$

where the last three terms are the non-hydrostatic pressure effects that are typically neglected in the SVE.

Viscous term

The remaining term in eq. (16) is the viscous term, which is treated as an empirical function in all but the most highly-resolved models of simple systems (note that Decoene et al. (2009) provides a comprehensive and rigorous approach for friction that has not yet been fully considered in SVE models). For the present purposes, we will retain the simple friction slope form with an assumption of linear behavior over space, i.e.

$$\oint_S \nu\frac{\partial u_j}{\partial x_k}\hat{i}_j n_k\,dA = -g\int_{V_e} S_f(x)\,dV \approx -gV_e S_{f(e)} \tag{43}$$

where $S_{f(e)}$ is the average friction slope over the control volume V_e.

Finite-volume for momentum

Putting together the above, eq. (16) can be written in a finite-volume form as

$$\frac{\partial}{\partial t}\left(U_e V_e\right) = \mathrm{sgn}(U_u)\,\beta_u Q_u U_u\cos\psi_u - \mathrm{sgn}(U_d)\,\beta_d Q_d U_d\cos\psi_d + \frac{1}{\rho}A_u P_u\cos\psi_u - \frac{1}{\rho}A_d P_d\cos\psi_d$$
$$+\frac{1}{\rho}\left(A_d\cos\psi_d - A_u\cos\psi_u\right)\int_L P(x)\lambda(x)\,dx - \frac{\cos\psi_u}{\rho}\int_{A_u}\breve{P}(x,y,z)\,dA + \frac{\cos\psi_d}{\rho}\int_{A_d}\breve{P}(x,y,z)\,dA$$
$$-\frac{1}{\rho}\int_L\gamma(x)\int_{A_R}\breve{P}(x,y,z)\,dA\,dx - gV_e S_{f(e)} + M_e \tag{44}$$

where U_e is the element velocity and V_e is the element volume. Note that $Q > 0$ and $U > 0$ imply flow in the nominal downstream direction, whereas $Q < 0$ and $U < 0$ imply flow in the nominal upstream direction. At this point we have introduced only five approximations: (1) uniform-density incompressibility, (2) the effect of channel curvature is either negligible or handled in an empirical viscous term, (3) the cross-channel variability in the free-surface slope is negligible, (4) the cross-channel variability in the bottom slope $\hat{\theta}(x,y)$ at any cross-section can be characterized by a single slope angle $\theta(x)$, and (5) a friction-slope model can be used to represented integrated viscous effects over a control volume. In addition we have a geometric restriction that the upstream and downstream control volume cross-sections must be vertical planes that are orthogonal (in the horizontal plane) to the mean flow direction.

For convenience in exposition, for the remainder of this paper we will apply the hydrostatic approximation ($\breve{P} = 0$) along with approximations for small slope ($\cos\psi \approx 1$), and uniform cross-section velocity ($\beta \approx 1$). Furthermore, we will limit our focus to flows without lateral momentum sources ($M_e = 0$), and without flow reversals ($\text{sgn}(U) = +1$). These simplifications allow us focus attention on the pressure source term, which is the primary new contribution in this derivation. The resulting simplification of eq. (44) can be presented with conservative terms on the LHS and source terms on the RHS as

$$\frac{\partial}{\partial t}(U_e V_e) - \frac{Q_u^2}{A_u} + \frac{Q_d^2}{A_d} - gA_u\eta_u + gA_d\eta_d = g(A_d - A_u)\int_L \eta(x)\lambda(x)\,dx - gV_eS_{f(e)} \tag{45}$$

where definition of piezometric pressure, eq. (23), is used to substitute $P = \rho g\eta$. A more formal finite-volume integral presentation would be

$$\frac{\partial}{\partial t}\int_V u\,dV - \int_{A_u} u^2\,dA + \int_{A_d} u^2\,dA - g\int_{A_u}\eta\,dA + g\int_{A_d}\eta\,dA = g(A_d - A_u)\int_L \eta(x)\lambda(x)\,dx - g\int_V S_f\,dV \tag{46}$$

Equation (45) can be reduced to a differential equation using $V = AL$ as $L \to 0$. Dividing through by L and taking the limit as $L \to 0$ provides

$$\frac{\partial Q}{\partial t} + \frac{\partial}{\partial x}\left(\frac{Q^2}{A} + gA\eta\right) = g\eta\frac{\partial A}{\partial x} - gAS_f \tag{47}$$

If we substitute geometric identities $\eta \equiv H + z_b$ and $S_0 \equiv -\partial z_b/\partial x$, we see that the above becomes identical to eq. (8). Thus, our finite-volume derivation is exactly consistent with the commonly-used differential SVE that is posed using S_0. However, from eqs. (45) and (47) we see that the free-surface source term in the differential form, $g\eta\,\partial A/\partial x$, is related to the more interesting integral source term in the finite-volume form:

$$g(A_d - A_u)\int_L \eta(x)\lambda(x)\,dx$$

This term can be thought of as an integrated free-surface/topography term that reflects nonlinearity in both the free surface and topography over a control volume. It is clear that this finite-volume term collapses to $g\eta\,\partial A/\partial x$ as $L \to 0$ but the integral form is not readily inferred from the differential form. Through approximations of this integral term we can obtain a variety of different finite-volume forms of the SVE, as outlined in the following section.

5 Approximate finite-volume forms of the SVE

General form

We are interested in approximate forms of the finite-volume SVE that arise from discretization choices in the integral source term derived above, so for exposition it will be convenient to start from the approximate form in eq. (45) with $V_e = A_eL_e$ and $Q_e = A_eU_e$. These approximations can be readily reversed to provide a more complete equation, but the simple form for further analysis is

$$L_e\frac{\partial Q_e}{\partial t} - \frac{Q_u^2}{A_u} + \frac{Q_d^2}{A_d} - gA_u\eta_u + gA_d\eta_d = T_e - gV_eS_{f(e)} \tag{48}$$

where T_e is the source term for integrated free-surface/topography effects obtained from the RHS of eq. (45):

$$T_e \equiv g\,(A_d - A_u) \int_L \eta(x)\lambda(x)\,dx \tag{49}$$

Note that the the LHS of eq. (48) is discretely conservative in that a summation over all elements will cause all the LHS terms to identically vanish except for the $\partial/\partial t$ and boundary conditions. Thus, the RHS are source terms, i.e. the traditional friction term and a term representing nonlinearities in the free surface interacting with topography can create and destroy momentum. The system is inherently "well-balanced" as discussed in Section 3, as long as T_e identically vanishes for a flat free surface.

Equation (49) admits a wide variety of approximate equations, depending on the form chosen for the quadrature of $\eta(x)$ and $\lambda(x)$ over the length of a finite volume. Arguably, a simple finite-volume discrete method will have three values of η that characterize a control volume: η_u, η_e, and η_d, as illustrated in Fig. 1. Different numerical methods can be constructed by using different approximations constructed from these three values. Herein, we cannot exhaustively investigate the variety of options and so will focus on the most obvious candidates, which are polynomials of orders 0 through 2. The zero-order polynomial is an approximation of $\eta(x)$ as a uniform value over the element length (e.g., as in the Godunov conceptual model, discussed in Section 3) – which could be simply represented by $\eta(x) = \eta_e$ so that the face values of η_d and η_u are ignored. Note that even this choice has alternate forms – a slightly different scheme could be constructed using $\eta(x) = (\eta_u + \eta_d)/2$, which is also uniform but ignores η_e. A first-order polynomial for $\eta(x)$ implies a linear free-surface slope across the element, which might be represented by a slope from η_d to η_u. A second-order polynomial implies a quadratic curvature to the free surface that can pass smoothly through η_u, η_e, and η_d. Clearly this idea could be extended to cubic splines by including adjacent control volume values. Beyond these polynomials there are other options that might be suitable. For example, we could use the three discrete η values to provide piecewise linear slopes from η_u to η_e and η_e to η_d. The open-ended nature of the $\eta(x)$ discretization should allow future development of a variety of finite-volume forms that can be easily demonstrated to be well-balanced and consistent with the above derivations.

By its definition in eq. (38) with constraint eq. (39), the weighting function $\lambda(x)$ is an abstraction of the distribution of changes in the pressure contribution from cross-sectional area parallel to the free surface, which is affected by both topography and the local slope of the free surface, as illustrated in Figs. 3 through 5. The $\lambda(x)$ is more complicated and abstract than $\eta(x)$ because the free-surface elevation is approximated as uniform at any x location, but $\lambda(x)$ represents the integrated effect of complex 3D topography, e.g. the $A_{R(m)}$ stair-step as illustrated in Fig. 6. The key point is that the $\lambda(x)$ weighting function has an integral constraint $\int \lambda\,dL = 1$ because the change in the cross-sectional area over the control volume, $A_d - A_u$, has already been extracted from the integral of PA_R through eq. (40). A comparison of Figs. 4 and 5 shows that $\lambda(x)$ is *not* independent of $\eta(x)$ and hence arguably should be a moderator between the static topography and the dynamics of the free surface. However, development of $\lambda(x,t)$ forms that are dynamically dependent on $\eta(x,t)$ are beyond the scope of the present work. Herein, we appeal to Occam's razor and note that the simplest $\lambda(x)$ that satisfies the integral constraint is $\lambda(x) = L_e^{-1}$, where L_e is the control volume length, illustrated in Fig. 1. This choice of $\lambda(x)$ is a zero-order polynomial implying the stair-steps are uniformly distributed over the element, as illustrated in Fig. 3. Clearly, for the nonlinear cases in Figs. 4 and 5 this form of $\lambda(x)$ is an approximation that reduces nonlinear interaction between the free surface and the topography. Arguably, this is

consistent with a discrete scheme using a single-valued geometry function such as $\eta_e = f(V_e)$ that neglects the effect of the free surface slope on the relationship between volume and surface elevation. Note that because the $A_d - A_u$ area is already extracted from the integral, using $\lambda(x) = L_e^{-1}$ ensures that the T_e term is exact at the linear limit and a bounded approximation for nonlinear interactions. That is, with $\lambda(x) = L_e^{-1}$ it follows that

$$T_e = \frac{g\,(A_d - A_u)}{L_e} \int_L \eta(x)\,dx \leq g\,(A_d - A_u) \max\left(\eta(x)\right)$$

Thus, the largest possible value for the T_e term is based on the maximum piezometric pressure over the control volume acting on the difference between upstream and downstream areas.

The simple form of $\lambda(x) = L^{-1}$ is consistent with either increasing cross-sectional area ($\gamma(x) > 0$ over L_e) or decreasing cross-sectional area ($\gamma(x) < 0$ over L_e), but is questionable for a non-monotonic case (e.g., Fig. 5). To examine this issue in more detail, consider the somewhat simpler case of a linear free surface slope with cross-sectional area that increases along the streamwise direction in the upper section and decreases in the lower, as shown in Fig. 7. The $\lambda(x) = L^{-1}$ approach cannot represent the actual change in cross-section area, but instead provides a linear trend between A_u and A_d as shown in Fig. 8. In contrast, if the control volume in Fig. 7 were split into two separate volumes at the centerline (i.e., the gray dashed lined), then the stair-steps of Fig. 7 would be readily represented by the $\lambda(x) = L^{-1}$ approximation as both control volumes would be monotonic.

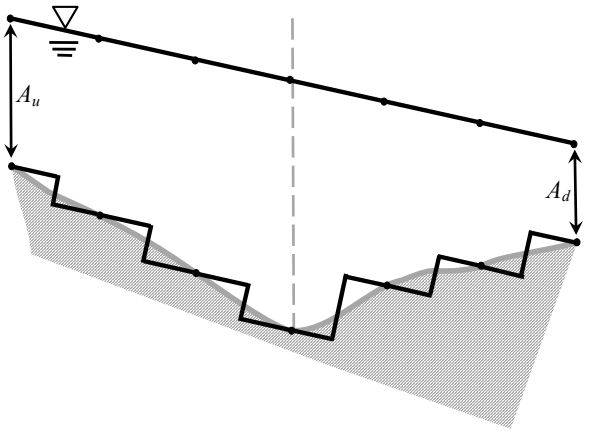

Figure 7. Non-monotonic stair-steps of cross-sectional area with linear monotonic free surface. Gray dashed line is where the cross-section area reverses from increasing to decreasing.

Comprehensive investigation of different forms for $\eta(x)$ and $\lambda(x)$ in the T_e term is clearly needed and will take significant future effort. For the present purposes, we examine the simplest polynomial forms for $\eta(x)$ in combination with the zeroth-order $\lambda(x) = L^{-1}$. To provide insight into how a higher-order $\lambda(x)$ discretization adds complexity in the derivation, we can

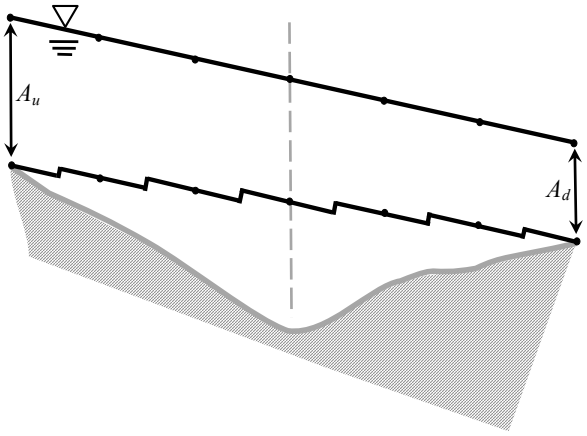

Figure 8. Approximated finite-element cross-section characteristics using $\lambda(x) = L_e^{-1}$ for non-monotonic topography in Fig. 7. Gray dashed line is where the cross-section area reverses from increasing to decreasing.

derive a simple linear form of $\lambda(x)$ that depends only on topography and couple with a linear form of $\eta(x)$. Such a $\lambda(x)$ is unlikely to be useful with a dynamic free surface, but is illustrative of the complexity that can be developed with quadrature of linear equations. We will use the nomenclature $T_{e(m,n)}$ to designate and m-order polynomial for $\eta(x)$ and an n-order polynomial for $\lambda(x)$.

The $T_{e(0,0)}$ approximation

The simplest approximations arise by assuming uniform values such that $\eta(x) \approx \bar{\eta}$ and $\lambda(x) \approx L_e^{-1}$, where $\bar{\eta}$ is the average water surface elevation over the element and we recall that $\int_L \lambda \, dx = 1$. It follows that

$$T_{e(0,0)} \equiv g\,(A_d - A_u)\,\bar{\eta} \tag{50}$$

If we let $\eta_e \approx \bar{\eta}$, then eq. (48) can be written as

$$L_e \frac{\partial Q_e}{\partial t} - \frac{Q_u^2}{A_u} + \frac{Q_d^2}{A_u} - gA_u\eta_u + gA_d\eta_d = g\,(A_d - A_u)\,\eta_e - gV_eS_{f(e)} \tag{51}$$

Note that the RHS in the above is what we might infer as a discrete finite-volume version of $g\,\eta\,\partial A/\partial x$ in the differential source term of eq. (47).

The $T_{e(1,0)}$ approximation

If we represent the free surface by a 1st-order polynomial, $\eta(x) = ax + b$, while retaining the zeroth-order $\lambda(x) = L_e^{-1}$ we obtain

$$T_{e(1,0)} = g\left(A_d - A_u\right)\left(\frac{aL}{2} + b\right) \tag{52}$$

A linear approximation is consistent with a free surface where $b = \eta_u$ and $a = -\left(\eta_u - \eta_d\right)/L$, so we obtain a finite-volume source term

$$T_{e(1,0)} = \frac{1}{2} g\left(A_d - A_u\right)\left(\eta_u + \eta_d\right) \tag{53}$$

Note that the above implies products of $A_d\eta_d$ and $A_u\eta_u$ in the source term that can be moved to the LHS as part of the conservative flux terms. Substituting $T_{e(1,0)}$ for T_e in eq. (48) and redistributing terms provides

$$L_e\frac{\partial Q_e}{\partial t} - \frac{Q_u^2}{A_u} + \frac{Q_d^2}{A_u} - \frac{1}{2}gA_u\eta_u + \frac{1}{2}gA_d\eta_d = \frac{1}{2}g\left(A_d\eta_u - A_u\eta_d\right) - gV_eS_{f(e)} \tag{54}$$

Thus, the model of a linear free surface and uniform $\lambda(x)$ serves to change the weighting of the $gA\eta$ terms (from unity to $1/2$) and provides a source term that contains only face values of A and η, which is unlike eq. (51) that requires an element approximation of η_e. Interestingly, the above finite-volume form does *not* have a differential representation as $L \to 0$. That is, the free-surface differential source term in eq. (47) is based on $(A_d - A_u)/L \to dA/dx$ as $L \to 0$. However, once we have chosen relationships for $\eta(x)$ and $\lambda(x)$ and moved a portion of the source term into the fluxes, an attempt to create a differential out of our source term encounters the form

$$\lim_{L\to 0}\frac{A_d\eta_u - A_u\eta_d}{L_e}$$

which can only be reduced to a differential by making additional approximations as to the behavior of A and η at the faces of the finite volume. For the special case of a rectangular channel with frictionless flow, eq. (54) can be transformed by using $A = BH$ where B is the breadth and H is the depth, so that we obtain a finite volume form of

$$L_e\frac{\partial}{\partial t}\left(H_eU_e\right) - H_uU_u^2 + H_dU_d^2 + \frac{1}{2}g\left(H_d^2 - H_u^2\right) = g\frac{\left(H_d + H_u\right)}{2}\left(z_u - z_d\right) \tag{55}$$

As $L_e \to 0$, and $S_0 = -\partial z/\partial x$, the above implies a conservative differential form of

$$\frac{\partial HU}{\partial t} + \frac{\partial}{\partial x}\left(HU^2\right) + \frac{1}{2}g\frac{\partial H^2}{\partial x} = gHS_0 \tag{56}$$

which is commonly used in studies of simplified conservative forms (e.g., Bouchut et al., 2003; Hsu and Yeh, 2002). Thus the $T_{e(1,0)}$ is also consistent with prior differential forms.

The $T_{e(2,0)}$ approximation

We can take this approach further by approximating the free surface as a parabola based on $\{\eta_u, \eta_e, \eta_d\}$ where η_e is a characteristic free surface height at the center of the finite volume. Using $\eta(x) = ax^2 + bx + c$ with $x = 0$ at A_u and $x = L$ at A_d, provides

$$c = \eta_u \tag{57}$$

$$b = \frac{1}{L}\left(-3\eta_u + 4\eta_e - \eta_d\right) \tag{58}$$

$$a = \frac{2}{L^2}\left(\eta_u - 2\eta_e + \eta_d\right) \tag{59}$$

Using $\lambda(x) = L^{-1}$, results in

$$T_{e(2,0)} = \frac{g}{6}\left(A_d - A_u\right)\left(\eta_u + 4\eta_e + \eta_d\right) \tag{60}$$

It is useful to multiply through and regroup terms so that $A_d\eta_d$ and $A_u\eta_u$ are isolated. Where these terms are balanced, they can be moved to the LHS as conservative terms. Regrouping provides:

$$T_{e(2,0)} = \frac{g}{6}\left\{A_d\eta_d - A_u\eta_u + A_d\left(\eta_u + 4\eta_e\right) - A_u\left(4\eta_e + \eta_d\right)\right\} \tag{61}$$

So our momentum equation can be written as

$$L_e\frac{\partial}{\partial t}\left(Q_e\right) - \frac{Q_u^2}{A_u} + \frac{Q_d^2}{A_d} - \frac{5}{6}gA_u\eta_u + \frac{5}{6}gA_d\eta_d = \frac{1}{6}g\left\{A_d\left(\eta_u + 4\eta_e\right) - A_u\left(4\eta_e + \eta_d\right)\right\} - gV_eS_{f(e)} \tag{62}$$

Once again, the specific representation of $\eta(x)\lambda(x)$ provides a modification of the coefficient of the $gA\eta$ terms in the conservative fluxes and sets the form of the non-conservative source term. This form does not appear to readily reduce to any differential form that is previously seen in the literature, and thus provides an interesting new avenue for investigation.

The $T_{e(1,1)}$ approximation

The above forms used a uniform $\lambda(x) = L^{-1}$. We can readily extend the concept to analytical forms of $\lambda(x)$, although it is not clear that such increasing complexity will yield an advantage in the design of a numerical model. The $\lambda(x)$ function is a weighting function that reflects distribution of the bottom elevation stair-steps, as described in §4. The only restriction on $\lambda(x)$ is that it must integrate to unity over L_e. Physically, as illustrated in Figs. 3 through 5, the $\lambda(x)$ should be a function of $\eta(x)$ as well as the topography. However, we do not (as yet) have a good working framework for a dynamic representation of $\lambda(x,\eta)$. Thus, to illustrate the complexities that arise with a non-uniform $\lambda(x)$, herein we will simply analyze a somewhat arbitrary static linear relationship where $\lambda(x) = \alpha z(x)$, where z is the bottom elevation and α is a scaling constant to ensure $\int_L \lambda\, dx = 1$. We introduce linear approximations of the bottom as $z(x) = Ax + B$ and the free surface as $\eta(x) = ax + b$. We

can write these approximations as

$$z(x) = -\frac{1}{L}(z_u - z_d)\,x + z_u \tag{63}$$

$$\eta(x) = -\frac{1}{L}(\eta_u - \eta_d)\,x + \eta_u \tag{64}$$

Using $\int_L \alpha z(x) = 1$, it can be shown that

$$\alpha = \frac{2}{L(z_u + z_d)} \tag{65}$$

Using eq. (49), a quadrature problem can be presented as

$$\begin{aligned}\frac{T_{e(1,1)}}{g(A_d - A_u)} &= \alpha \int_L z(x)\eta(x)\,dx \\ &= \frac{2}{L(z_u + z_d)} \int_L \left[-\frac{1}{L}(z_u - z_d)\,x + z_u\right]\left[-\frac{1}{L}(\eta_u - \eta_d)\,x + \eta_u\right] dx\end{aligned} \tag{66}$$

After some algebra, we find

$$\frac{T_{e(1,1)}}{g(A_d - A_u)} = \frac{2\eta_u z_u + \eta_u z_d + \eta_d z_u + 2\eta_d z_d}{3(z_u + z_d)} \tag{67}$$

Unfortunately, for the above form we cannot use the redistribution trick to split T_e and move a portion to the LHS of eq. (48). The problem is that any split term will have $z_u + z_d$ in the denominator, which will not be conservative when used as a coefficient on a control volume face. Thus, the $T_{e(1,1)}$ form of momentum is

$$L_e\frac{\partial Q_e}{\partial t} - \frac{Q_u^2}{A_u} + \frac{Q_d^2}{A_u} - gA_u\eta_u + gA_d\eta_d = g(A_d - A_u)\left(\frac{2\eta_u z_u + \eta_u z_d + \eta_d z_u + 2\eta_d z_d}{3(z_u + z_d)}\right) - gA_e S_{f(e)} \tag{68}$$

In general, it appears that only the uniform $\lambda(x) = L_e^{-1}$ form will allow us to shift of part of the source term onto the flux side. Any form that has a non-uniform $\lambda(x)$ must necessarily have a dependency on $z(x)$ in the cell to satisfy $\int_L \lambda\,dx = 1$. We cannot create a conservative term at a face when the value computed from the downstream cell depends on a value within the downstream volume and while the value computed from the upstream cell depends on a value within the upstream volume. Note that this particular $T_{e(1,1)}$ form is for demonstration purposes and is *not* recommended for use in any numerical scheme. This $T_{e(1,1)}$ is predicated on an assumed weighting of $\lambda(x) = \alpha z(x)$, which does not have a physical linkage to specific cross-section geometry or expected flow conditions.

Summary of approximate forms

The $T_{e(0,0)}$, $T_{e(1,0)}$, $T_{e(2,0)}$ and $T_{e(1,1)}$ approximations all follow a similar form

$$L_e\frac{\partial Q_e}{\partial t} - \frac{Q_u^2}{A_u} + \frac{Q_d^2}{A_d} - gA_u\eta_u(1 - \delta_u) + gA_d\eta_d(1 - \delta_d) = K_{e(m,n)} - gV_e S_{f(e)} \tag{69}$$

where $0 \le \delta_u, \delta_d \le 1$ are fixed coefficients and $K_{e(m,n)}$ is a time-space-varying topographic source term, whose exact forms are determined by the approximations used for T_e. This form was suggested in Section 2 with eq. (9) based on a philosophical

Table 2. Values for conservative $A\eta$ coefficients and $K_{e(m,n)}$ source terms for finite volume schemes with (m,n) polynomial approximations of T_e. Note that forms using $(m,n)=(m,1)$ are not recommended without further theoretical development and are provided only for illustrative purposes.

(m,n)	$\delta_{u(m,n)}$	$\delta_{d(m,n)}$	$K_{e(m,n)}$
$(0,0)$	0	0	$g\left(A_d - A_e\right)\eta_e$
$(1,0)$	$1/2$	$1/2$	$g\left(A_d\eta_u - A_u\eta_d\right)/2$
$(2,0)$	$1/6$	$1/6$	$g\left\{A_d\left(\eta_u + 4\eta_e\right) - A_u\left(\eta_d + 4\eta_e\right)\right\}/6$
$(1,1)$	0	0	$g\left(A_d - A_u\right)\left(\frac{2\eta_u z_u + \eta_u z_d + \eta_d z_u + 2\eta_d z_d}{3(z_u + z_d)}\right)$

argument of moving as much as possible of the RHS source terms to the conservative LHS flux terms. The key point for future work is that these forms (with the exception of $K_{e(1,1)}$) are relatively straightforward in their representation of values that are the natural elements of a SVE computational model for river networks and urban drainage. This approach eliminates the need for estimating or computing the I_1 and I_2 of the Cunge-Liggett conservative form and replaces them with the simple cross-sectional area term and a K_e that is computed from discrete values of η, and A. Values for δ_u, δ_d and K_e for these forms are presented in Table 2. Examination of the above leads to the conclusion that the use of any polynomial representation of $\eta(x)$ with $\lambda(x) = L^{-1}$ will produce a $K_{e(m,0)}$ source term that will exactly vanish when the free surface is flat, e.g., $\eta_u = \eta_e = \eta_d$. Thus, these schemes are inherently "well-balanced" as discussed in Section 3. Furthermore, for these cases the source terms will be Lipschitz smooth as long as the solution variables are smooth.

6 Discussion

The complete differential form of the non-hydrostatic version of the Saint-Venant equations, simplified from the derivation in Section 4, can be written as

$$\frac{\partial Q}{\partial t} + \frac{\partial}{\partial x}\left(\left[\beta\frac{Q^2}{A} + gA\eta + \frac{\breve{P}}{\rho}\right]\cos\psi\right) = g\eta\frac{\partial A}{\partial x}\cos\psi + \frac{1}{\rho}\int_{A_R}\breve{P}(z)dA - gAS_f + m_e \tag{70}$$

which is similar to previous work but includes both non-hydrostatic terms and effects of free surface slope ($\cos\psi$) that are often neglected. The key contribution of the present work is the semi-discrete, conservative, finite-volume form that corresponds to the differential form above:

$$\begin{aligned}
&\frac{\partial}{\partial t}\left(U_e V_e\right) - \operatorname{sgn}(Q_u)\,\beta_u \frac{Q_u^2}{A_u}\cos\psi_u + \operatorname{sgn}(Q_d)\,\beta_d \frac{Q_d^2}{A_d}\cos\psi_d \\
&- gA_u\eta_u\cos\psi_u + gA_d\eta_d\cos\psi_d - \frac{\cos\psi_u}{\rho}A_u\breve{P}_u + \frac{\cos\psi_d}{\rho}A_d\breve{P}_d \\
&\quad = g\left(A_d\cos\psi_d - A_u\cos\psi_u\right)\int_L \eta(x)\lambda(x)\,dx + \frac{1}{\rho}\int_L \gamma(x)\int_{A_R}\breve{P}(x,y,z)\,dA\,dx - gV_eS_{f(e)} + M_e
\end{aligned} \tag{71}$$

where $\breve{P}_u$ and $\breve{P}_d$ are the average non-hydrostatic pressures on the upstream and downstream cross-sectional areas. In this finite-volume form, the only approximations introduced are: (1) uniform-density incompressibility, (2) the effects of momentum redirection around bends is either negligible or is handled in friction terms, (3) the cross-channel variability in the free-surface slope is negligible, (4) the cross-channel variability in the bottom slope at any cross-section can be reasonably represented by a single slope angle $\theta(x)$, and (5) a friction slope model can be used to represented integrated viscous effects. In addition we have introduced a geometric restriction that the upstream and downstream cross-sections must be vertical planes that are orthogonal (in the horizontal plane) to the mean flow direction. The above form can be used to analyze systems that include non-hydrostatic pressure and slope gradients beyond the small-slope approximation of the traditional SVE. As warning for future development of non-hydrostatic methods, note that the fundamental 1D derivation is effectively treating the non-hydrostatic pressure gradients in the horizontal as absorbing and redirecting momentum along the curving channel. Thus a part of the this term is, in effect, encapsulated within the approximation that allows A_u and A_d to be cross-sections that are not parallel.

The principal feature of the new finite-volume formulation is the topographic source term $\int \eta(x)\lambda(x)\,dx$ that can be represented by analytical functions to approximate a smoothly-varying free surface and its interaction with topography across the finite-volume element. Discrete polynomial representations of $\int \eta(x)\lambda(x)\,dx$ have been evaluated in Section 5, with the resulting topographic terms designated as $T_{e(m,n)}$ for an m-degree polynomial representing η and an n-degree polynomial representing λ. In an approximate form, the $T_{e(m,n)}$ term is split into a $\delta_{u(m,n)}$ factor applied to $gA_u\eta_u$ and a $\delta_{d(m,n)}$ factor applied to $gA_d\eta_d$, which become part of the conservative flux terms. The remainder of the $T_{e(m,n)}$ becomes a $K_{e(m,n)}$ source term in the approximate finite-volume form. Simpler conservative finite-volume forms that use the common approximations of the hydrostatic equations ($\breve{P} \approx 0$) with small free surface slope ($\cos\psi \approx 1$), uniform cross-sectional velocity ($\beta \approx 1$), non-reversing flow ($\operatorname{sgn}(U) = +1$), no momentum sources ($M_e = 0$), can be written as

$$L_e\frac{\partial Q_e}{\partial t} - \frac{Q_u^2}{A_u} + \frac{Q_d^2}{A_d} - gA_u\eta_u\left(1-\delta_{u(m,n)}\right) + gA_d\eta_d\left(1-\delta_{d(m,n)}\right) = K_{e(m,n)} - gL_eA_eS_{f(e)} \tag{72}$$

where the discrete K_e and δ terms are shown in Table 2. It is worthwhile to compare the above to a finite-volume form derived using the Cunge-Liggett form of the SVE, which could be written (using the I_1 and I_2 definitions) as

$$L_e\frac{\partial Q}{\partial t} - \frac{Q_u^2}{A_u} + \frac{Q_d^2}{A_d} - g\int_{H(u)}(H-z)\,B(z)\,dz + g\int_{H(d)}(H-z)\,B(z)\,dz = g\int_L\int_H (H-z)\frac{\partial B}{\partial x}\,dx + g\int_L A\left(S_0 - S_f\right)dx \tag{73}$$

Performance of the traditional scheme depends on the specification for $B(x,z)$ that defines the irregular bathymetry of the channel. Although the $B(x,z)$ term is developed without any approximations, it is a non-trivial matter to simplify these terms to create practical computational forms for irregular cross-section geometry. The source term on the RHS of the Cunge-Liggett form is effectively an integration of both variations in the channel topography and the water surface elevation over the volume length L_e that does not have a limiting constraint. Furthermore, the selection of $B(x,z)$ for the RHS affects the integration on the LHS hydrostatic pressure term – thus obtaining a "well-balanced" source term that compensates for S_0 will also affect the conservative flux terms. The $\lambda(x)$ used to develop the K_e term eq. (72) serves a similar purpose to the source-term integral in the Cunge-Liggett form, but provides a simple weighting function that can be analytically integrated with an approximation for $\eta(x)$ and is inherently constrained such that $\int \lambda \, dx = 1$ over a control volume. The other major difference between the two approaches is that eq. (73) uses S_0 as a source term on the RHS of the equations while the new approach, eq. (72) dispenses with this artifice so that the source terms only include friction (which is guaranteed to damp momentum) and the portion of the topographic effects that cannot be fit into the conservative δ_u and δ_d terms.

There is a long history of using of S_0 in a source term in the SVE, and it is indeed part of the author's prior model (Liu and Hodges, 2014). However, use of S_0 with irregular geometry brings the problems of creating a "well-balanced" conservative scheme, as discussed in Section 3. Furthermore, the use of S_0 in a source term requires the pressure term to be treated as the hydrostatic pressure rather than the piezometric pressure, as shown in Section 4. Because the hydrostatic pressure is a function of depth, its integration over an irregular cross-sectional area requires knowledge of the distribution of depth across the channel – a significant computational complexity. In contrast as shown in eq. (24), the integration of the piezometric pressure over a cross-section is exactly PA and does not require knowledge of how depth is distributed across the channel. Other authors have noted similar problems: Schippa and Pavan (2008) derived a conservative differential form that retained gI_1 in the flux terms and removed S_0 by showing that it could be combined with the I_2 source term as as $\partial I_1/\partial x$ for a uniform water level. It seems that the Schippa and Pavan (2008) differential equation might be preferred to the approach proposed herein for high-resolution topography with small grid spacing (i.e., where we have confidence that the computation of I_1 is meaningful). However, at larger scales where geometric cross-sections are broadly spaced and the computation of I_1 is questionable, the simplicity of using A and η for piezometric pressure gradient terms is likely to be preferred. Other authors, notably Rosatti et al. (2011), have simply accepted $gA\partial\eta/\partial x$ as an unavoidable source term rather than dealing with the problems of obtaining a well-balanced method with the hydrostatic pressure.

Since S_0 was not in Alexandre de Saint-Venant's original paper, how it come to be commonly used in the Saint-Venant equations? Arguably there are two sources associated with different simulation scales: (1) in hydrology the kinematic wave model provides $S_0 = S_f$, which leads to prioritization of S_0 as a hydraulic parameter, and (2) in mathematics the equation:

$$\frac{\partial hu}{\partial t} + \frac{\partial hu}{\partial x} = s \tag{74}$$

is the canonical form of a 1D inhomogenous hyperbolic advection equation for depth h and velocity u, which leads to a prioritization of the depth as a fundamental parameter and requires $S_0(x)$ be relegated to the source term for irregular geometry. However, for solution of the SVE there is no need to exactly mimic the hyperbolic advection equation to obtain a conservative

form, thus there is no need to introduce S_0. The above comparisons of the Cunge-Liggett form and the new finite-volume form illustrate the additional complexity of introducing S_0 in the finite-volume form. Beyond these issues is a more fundamental problem: numerical methods for inhomogeneous partial differential equations are only well-posed if the source terms are Lipschitz smooth (Iserles, 1996) – otherwise one should not be surprised by numerical instabilities and/or difficulties in convergence. Any river model that uses raw data from surveyed cross-sections will inherently have non-smooth $S_0(x)$. As a result, much of the computational complexity is likely to be compensating for the lack of Lipschitz smoothness in the boundary conditions of topography. In contrast, when the surface elevation (piezometric pressure) is used instead of depth (hydrostatic pressure), then $S_0(x)$ disappears from the SVE and the smoothness of the source term is assured (for a smooth solution) by the choice of smooth functions for $\lambda(x)$ and $\eta(x)$ and the friction slope model $S_f(x)$. In general, as long as the solutions of η and Q remain smooth the source term of the SVE derived herein should remain smooth. That is, the approach herein cannot guaranty a smooth solution, but it can guaranty that any observed non-smoothness in the source terms during a simulation is a result of non-smoothness in the solution rather than direct forcing of boundary conditions.

As a matter of pure speculation, the new form of the finite-volume equations brings up some interesting possibilities for large-scale modeling. Imagine that we would like to model a river network or urban drainage network where we have some high-resolution (1×1 m) data in some areas but not in others. Let us also say our computer power limits us to a SVE solution with a median cell length of about 20 m. Can we incorporate our high resolution knowledge directly at the coarse scale? Arguably, the $\lambda(x)$ approach could give us a means of directly incorporating effects of subgrid scale topography into a single source term – however, significant theoretical work needs to be undertaken to develop a consistent methodology that is both "well-balanced" and Lipschitz smooth.

Clearly, there remains much practical experimentation to be done in comparing various forms of $T_{e(m,n)}$ and the effectiveness of different numerical solution methods with different $\eta(x)$ polynomial representations. There is also a need to develop a firm theoretical relationship between $\lambda(x)$ to $\eta(x)$ to overcome the difficulties illustrated with Figs. 4 and 5 where nonlinear interactions between the free surface and topography cannot be readily represented with the uniform $\lambda(x) = L^{-1}$ applied herein. Finally, there are substantial questions on whether the new approach can be used with methods designed to satisfy the entropy criterion (e.g. Greenberg and Leroux, 1996; Harten et al., 1983; Lax, 1973). It is hoped that researchers will consider adapting their finite-volume codes to the form of eq. (72) and reporting their experience.

7 Conclusions

New finite-volume forms of integral momentum equations for unsteady flow in open channels with varying cross-sections have been derived in this paper. These equations reduce to the classic differential forms of the Saint-Venant equations (under the $T_{e(0,0)}$ and $T_{e(1,0)}$ approximations) and also provide new approximate finite-volume forms that are suitable for analytical representations of topogarphy and free surface elevation over a finite-volume element. The new forms use the piezometric pressure (free surface elevation) rather than hydrostatic pressure (depth) as a fundamental variable, and thus do *not* include the channel slope, S_0. This approach provides a cleaner finite-volume form as the nonlinear interactions of topography and the free

surface are handled in a single integral term, $g\left(A_d - A_u\right) \int \eta \lambda \, dx$ where λ is a quadrature weighting function. This approach provide a venue to convert practical knowledge of fluid/geometry variations within the finite volume into source and flux terms of the finite-volume equations. This is a new approach to generating a variety of conservative, well-balanced, finite-volume forms for the SVE that could be employed in a wide range of numerical schemes. This work provides only the theoretical development for the new finite-volume approach. The practical implementation and numerical testing remains a subject for future work.

Code availability. A demonstration code for discretized application of the new SVE form is available on GitHub at https://github.com/benrhodges/SvePy. This code is associated with a companion paper Hodges and Liu (2018) that explains the discretized form.

Competing interests. The author declares that he has no conflicts of interest.

Acknowledgements. This article was developed under Cooperative Agreement No. 83595001 awarded by the U.S. Environmental Protection Agency to The University of Texas at Austin. It has not been formally reviewed by EPA. The views expressed in this document are solely those of the author and do not necessarily reflect those of the Agency. EPA does not endorse any products or commercial services mentioned in this publication.

References

Abbott, M. B. and Ionescu, F.: On The Numerical Computation Of Nearly Horizontal Flows, Journal of Hydraulic Research, 5, 97–117, https://doi.org/10.1080/00221686709500195, 1967.

Arico, C. and Tucciarelli, T.: A marching in space and time (MAST) solver of the shallow water equations. Part I: The 1D model, Advances in Water Resources, 30, 1236–1252, https://doi.org/10.1016/j.advwatres.2006.11.003, 2007.

Audusse, E., Bouchut, F., Bristeau, M.-O., Klein, R., and Perthame, B.: A Fast and Stable Well-Balanced Scheme with Hydrostatic Reconstruction for Shallow Water Flows, SIAM Journal on Scientific Computing, 25, 2050–2065, https://doi.org/10.1137/S1064827503431090, 2004.

Audusse, E., Bouchut, F., Bristeau, M.-O., and Sainte-Marie, J.: Kinetic Entropy Inequality and Hydrostatic Reconstruction Scheme for the Saint-Venant System, Mathematics Of Computation, 85, 2815–2837, https://doi.org/10.1090/mcom/3099, 2016.

Blanckaert, K. and Graf, W.: Momentum transport in sharp open-channel bends, Journal of Hydraulic Engineering-ASCE, 130, 186–198, https://doi.org/10.1061/(ASCE)0733-9429(2004)130:3(186), 2004.

Bollermann, A., Chen, G., Kurganov, A., and Noelle, S.: A Well-Balanced Reconstruction of Wet/Dry Fronts for the Shallow Water Equations, Journal Of Scientific Computing, 56, 267–290, https://doi.org/10.1007/s10915-012-9677-5, 2013.

Bouchut, F. and Morales de Luna, T.: A Subsonic-Well-Balanced Reconstruction Scheme For Shallow Water Flows, SIAM Journal on Numerical Analysis, 48, 1733–1758, https://doi.org/10.1137/090758416, 2010.

Bouchut, F., Mangeney-Castelnau, A., Perthame, B., and Vilotte, J.: A new model of Saint Venant and Savage-Hutter type for gravity driven shallow water flows, Comptes Rendus Mathematique, 336, 531–536, https://doi.org/10.1016/S1631-073X(03)00117-1, 2003.

Brunner, G. W.: HEC-RAS River Analysis System Hydraulic Reference Manual, US Army Corps of Engineers, Davis, CA USA, 2010.

Buntina, M. V. and Ostapenko, V. V.: TVD Scheme for Computing Open Channel Wave Flows, Computational Mathematics and Mathematical Physics, 48, 2241–2253, https://doi.org/10.1134/S0965542508120130, 2008.

Burger, G., Sitzenfrei, R., Kleidorfer, M., and Rauch, W.: Parallel flow routing in SWMM 5, Environmental Modelling & Software, 53, 27–34, https://doi.org/10.1016/j.envsoft.2013.11.002, 2014.

Canelon, D. J.: Pivoting Strategies in the Solution of the Saint-Venant Equations, Journal of Irrigation and Drainage Engineering-ASCE, 135, 96–101, 2009.

Casas, A., Lane, S. N., Yu, D., and Benito, G.: A method for parameterising roughness and topographic sub-grid scale effects in hydraulic modelling from LiDAR data, Hydrology and Earth System Sciences, 14, 1567–1579, https://doi.org/10.5194/hess-14-1567-2010, 2010.

Castellarin, A., Di Baldassarre, G., Bates, P. D., and Brath, A.: Optimal Cross-Sectional Spacing in Preissmann Scheme 1D Hydrodynamic Models, Journal of Hydraulic Engineering-ASCE, 135, 96–105, https://doi.org/10.1061/ASCE0733-94292009135:296, 2009.

Castro Diaz, M. J., Chacon Rebollo, T., Fernandez-Nieto, E. D., and Pares, C.: On well-balanced finite volume methods for nonconservative nonhomogeneous hyperbolic systems, SIAM Journal On Scientific Computing, 29, 1093–1126, https://doi.org/10.1137/040607642, 2007.

Catella, M., Paris, E., and Solari, L.: Conservative scheme for numerical modeling of flow in natural geometry, Journal of Hydraulic Engineering-ASCE, 134, 736–748, https://doi.org/10.1061/(ASCE)0733-9429(2008)134:6(736), 2008.

Chau, K. W. and Lee, J. H.: Mathematical modelling of Shing Mun River network, Advances in Water Resources, 14, 106–112, 1991.

Chen, A., Hsu, M., Chen, T., and Chang, T.: An integrated inundation model for highly developed urban areas, Water Science and Technology, 51, 221–229, 5th International Conference on Sustainable Techniques and Strategies in Urban Water (NOVATECH 2004), Lyon, FRANCE, JUN 06-10, 2004, 2005.

Cohen, S., Praskievicz, S., and Maidment, D. R.: Featured Collection Introduction: National Water Model, Journal of the American Water Resources Association, 54, 767–769, https://doi.org/10.1111/1752-1688.12664, 2018.

Crnković, B., Crnjarić-Zic, N., and Kranjcevic, L.: Improvements of semi-implicit schemes for hyperbolic balance laws applied on open channel flow equations, Computers & Mathematics with Applications, 58, 292–309, https://doi.org/10.1016/j.camwa.2009.04.004, 2009.

Cunge, J. A., Holly, F. M., and Verwey, A.: Practical Aspects of Computational River Hydraulics, Pitman Publishing Ltd, Boston MA, 1980.

David, C. H., Habets, F., Maidment, D. R., and Yang, Z. L.: RAPID applied to the SIM-France model, Hydrological Processes, 25, 3412–3425, https://doi.org/10.1002/hyp.8070, 2011.

David, C. H., Yang, Z.-L., and Hong, S.: Regional-scale river flow modeling using off-the-shelf runoff products, thousands of mapped rivers and hundreds of stream flow gauges, Environmental Modelling & Software, 42, 116 – 132, 2013.

de Saint-Venant, A. B.: Théorie du mouvement non permanent des eaux, avec application aux crues des rivières et à introduction des marées dans leurs lits, Comptes Rendus des Séances de l'Académie des Sciences, 73, 237–240, 1871.

Decoene, A., Bonaventura, L., Miglio, E., and Saleri, F.: Asymptotic derivation of the section-averaged shallow water equations for natural river hydraulics, Mathematical Models & Methods in Applied Sciences, 19, 387–417, 2009.

Delis, A. I. and Skeels, C. P.: TVD Schemes for Open Channel Flow, International Journal for Numerical Methods in Fluids, 26, 791–809, 1998.

Delis, A. I., Skeels, C. P., and Ryrie, S. C.: Implicit high-resolution methods for modelling one-dimensional open channel flow, Journal of Hydraulic Research, 38, 369–382, 2000a.

Delis, A. T., Skeels, C. P., and Ryrie, S. C.: Evaluation of some approximate Riemann solvers for transient open channel flows, Journal of Hydraulic Research, 38, 217–231, https://doi.org/10.1080/00221680009498339, 2000b.

Ferreira, V., de Queiroz, R., Lima, G., Cuenca, R., Oishi, C., Azevedo, J., and McKee, S.: A bounded upwinding scheme for computing convection-dominated transport problems, Computers & Fluids, 57, 208–224, https://doi.org/10.1016/j.compfluid.2011.12.021, 2012.

Gasiorowski, D.: Balance errors generated by numerical diffusion in the solution of non-linear open channel flow equations, Journal of Hydrology, 476, 384–394, https://doi.org/10.1016/j.jhydrol.2012.11.008, 2013.

Getirana, A., Peters-Lidard, C., Rodell, M., and Bates, P. D.: Trade-off between cost and accuracy in large-scale surface water dynamic modeling, Water Resources Research, 53, 4942–4955, 2017.

Godunov, S. K.: A difference method for numerical calculation of discontinuous solutions of the equations of hydrodynamics, Mathematicheskii Sbornik, 47, 271–306, http://www.mathnet.ru/links/f6aa08b1a9a1ef659306076fde997be3/sm4873.pdf, 1959.

Gottardi, G. and Venutelli, M.: Central schemes for open-channel flow, International Journal for Numerical Methods in Fluids, 41, 841–861, https://doi.org/10.1002/d.471, 2003.

Goutal, N. and Maurel, F.: A finite volume solver for 1D shallow-water equations applied to an actual river, International Journal for Numerical Methods in Fluids, 38, 1–19, 2002.

Greenberg, J. M. and Leroux, A. Y.: A well-balanced scheme for the numerical processing of source terms in hyperbolic equations, SIAM Journal on Numerical Analysis, 33, 1–16, 1996.

Guinot, V.: Upwind finite volume solution of sensitivity equations for hyperbolic systems of conservation laws with discontinuous solutions, Computers & Fluids, 38, 1697–1709, https://doi.org/doi:10.1016/j.compfluid.2009.03.002, 2009.

Gulbaz, S. and Kazezyilmaz-Alhan, C. M.: Calibrated Hydrodynamic Model for Sazlidere Watershed in Istanbul and Investigation of Urbanization Effects, Journal of Hydrologic Engineering, 18, 75–84, https://doi.org/10.1061/(ASCE)HE.1943-5584.0000600, 2013.

Harten, A., Lax, P. D., and Leer, B. V.: On upstream differencing and Godunov-type schemes for hyperbolic conservation laws, SIAM Review, 25, 35–61, 1983.

Hernandez-Duenas, G. and Beljadid, A.: A central-upwind scheme with artificial viscosity for shallow-water flows in channels, Advances in Water Resources, 96, 323–338, https://doi.org/10.1016/j.advwatres.2016.07.021, 2016.

Hodges, B. R.: Challenges in Continental River Dynamics, Environmental Modelling & Software, 50, 16–20, 2013.

Hodges, B. R. and Imberger, J.: Simple curvilinear method for numerical methods of open channels, Journal of Hydraulic Engineering-ASCE, 127, 949–958, https://doi.org/10.1061/(ASCE)0733-9429(2001)127:11(949), 2001.

Hodges, B. R. and Liu, F.: Rivers and Electric Networks: Crossing Disciplines in Modeling and Simulation, Foundations and Trends in Electronic Design Automation, 8, 1–116, 2014.

Hodges, B. R. and Liu, F.: No-neighbor discretization of a Saint-Venant model for unsteady open-channel flow, Journal of Hydraulic Research, (submitted June 2018), 2018.

Hsu, C.-T. and Yeh, K.-C.: Iterative explicit simulation of 1D surges and dam-break flows, International Journal for Numerical Methods in Fluids, 38, 647–675, https://doi.org/10.1002/d.236, 2002.

Hsu, M., Chen, S., and Chang, T.: Inundation simulation for urban drainage basin with storm sewer system, Journal of Hydrology, 234, 21–37, https://doi.org/10.1016/S0022-1694(00)00237-7, 2000.

Iserles, A.: A first course in the numerical analysis of differential equations, Cambridge University Press, Cambridge, UK, 1996.

Islam, A., Raghuwanshi, N. S., and Singh, R.: Development and application for irrigation of hydraulic simulation model canal network, Journal of Irrigation and Drainage Engineering-ASCE, 134, 49–59, https://doi.org/10.1061/ASCE0733-94372008134:149, 2008.

Ivanova, K., S.L. Gavrilyuk and, B. N., and Richard, G.: Formation and coarsening of roll-waves in shear shallow water flows down an inclined rectangular channel, Computers & Fluids, 159, 189–203, https://doi.org/10.1016/j.compfluid.2017.10.004, 2017.

Karelsky, K., Papkov, V., Petrosyan, A., and Tsygankov, D.: Particular solutions of shallow-water equations over a non-flat surface, PHYSICS LETTERS A, 271, 341–348, https://doi.org/10.1016/S0375-9601(00)00378-9, 2000.

Katsaounis, T., Perthame, B., and Simeoni, C.: Upwinding Sources at Interfaces in Conservation Laws, Applied Mathematics Letters, 17, 309–316, https://doi.org/10.1016/S0893-9659(04)00012-6, 2004.

Kesserwani, G., Mose, R., Vazquez, J., and Ghenaim, A.: A practical implementation of high-order RKDG models for the 1D open-channel flow equations, International Journal for Numerical Methods in Fluids, 59, 1389–1409, 2009.

Kesserwani, G., Ghostine, R., Vazquez, J., Ghenaim, A., and Mose, R.: Application of a second-order Runge-Kutta discontinuous Galerkin scheme for the shallow water equations with source terms, International Journal for Numerical Methods in Fluids, 56, 805–821, https://doi.org/10.1002/fld.1550, 2008.

Kesserwani, G., Liang, Q., Vazquez, J., and Mose, R.: Well-balancing issues related to the RKDG2 scheme for the shallow water equations, International Journal for Numerical Methods in Fluids, 62, 428–448, https://doi.org/10.1002/fld.2027, 2010.

Krebs, G., Kokkonen, T., Valtanen, M., Koivusalo, H., and Setala, H.: A high resolution application of a stormwater management model (SWMM) using genetic parameter optimization, Urban Water Journal, 10, 394–410, https://doi.org/10.1080/1573062X.2012.739631, 2013.

Kurganov, A. and Petrova, G.: A second-order well-balanced positivity preserving central-upwind scheme for the Saint-Venant system, Communications in Mathematical Sciences, 5, 133–160, 2007.

Lai, C., Baltzer, R. A., and Schaffranek, R. W.: Conservation-form equations of unsteady open-channel flow, Journal of Hydraulic Research, 40, 567–578, https://doi.org/10.1080/00221680209499901, 2002.

Lai, W. and Khan, A. A.: Discontinuous Galerkin Method for 1D Shallow Water Flows in Natural Rivers, Engineering Applications of Computational Fluid Mechanics, 6, 74–86, 2012.

Lax, P. D.: Hyperbolic Systems of Conservation Laws and the Mathematical Theory of Shock Waves, chap. 1, pp. 1–48, SIAM, https://doi.org/10.1137/1.9781611970562.ch1, 1973.

Leandro, J. and Martins, R.: A methodology for linking 2D overland flow models with the sewer network model SWMM 5.1 based on dynamic link libraries, Water Science and Technology, 73, 3017–3026, https://doi.org/10.2166/wst.2016.171, 2016.

Li, J. and Chen, G.: The generalized Riemann problem method for the shallow water equations with bottom topography, International Journal for Numerical Methods in Engineering, 65, 834–862, https://doi.org/10.1002/nme.1471, 2006.

Li, M., Guyenne, P., Li, F., and Xu, L.: A Positivity-Preserving Well-Balanced Central Discontinuous Galerkin Method for the Nonlinear Shallow Water Equations, Journal of Scientific Computing, 71, 994–1034, https://doi.org/10.1007/s10915-016-0329-z, 2017.

Liang, Q. and Marche, F.: Numerical resolution of well-balanced shallow water equations with complex source terms, Advances in Water Resources, 32, 873–884, https://doi.org/10.1016/j.advwatres.2009.02.010, http://linkinghub.elsevier.com/retrieve/pii/S0309170809000396, 2009.

Liggett, J. A.: Unsteady Flow in Open Channels, chap. 2: Basic equations of unsteady flow, Water Resources Publications, Fort Collins, Colorado, 1975.

Liu, F. and Hodges, B. R.: Applying microprocessor analysis methods to river network modeling, Environmental Modelling & Software, 52, 234–252, https://doi.org/10.1016/j.envsoft.2013.09.013, 2014.

Lyn, D. A. and Altinakar, M.: St. Venant–Exner Equations for Near-Critical and Transcritical Flows, Journal of Hydraulic Engineering-ASCE, 128, 579–587, https://doi.org/10.1061/ ASCE!0733-9429 2002!128:6 579!, 2002.

Mohamed, K.: A finite volume method for numerical simulation of shallow water models with porosity, Computers & Fluids, 104, 9–19, https://doi.org/10.1016/j.compfluid.2014.07.020, 2014.

Monthe, L., Benkhaldoun, F., and Elmahi, I.: Positivity preserving finite volume Roe schemes for transport-diffusion equations, Computer Methods In Applied Mechanics And Engineering, 178, 215–232, https://doi.org/10.1016/S0045-7825(99)00015-8, 1999.

Paiva, R. C. D., Collischonn, W., and Costa Buarque, D.: Validation of a full hydrodynamic model for large-scale hydrologic modelling in the Amazon, Hydrological Processes, 27, 333–346, 2013.

Paiva, R. C. D., Collischonn, W., and Tucci, C. E. M.: Large scale hydrologic and hydrodynamic modeling using limited data and a GIS based approach, Journal of Hydrology, 406, 170–181, https://doi.org/10.1016/j.jhydrol.2011.06.007, 2011.

Papanicolaou, A. N., Bdour, A., and Wicklein, E.: One-dimensional hydrodynamic/sediment transport model applicable to steep mountain streams, Journal of Hydraulic Research, 42, 357–375, 2004.

Paz, A. R., Bravo, J. M., Allasia, D., Collischonn, W., and Tucci, C. E. M.: Large-Scale Hydrodynamic Modeling of a Complex River Network and Floodplains, Journal of Hydrologic Engineering, 15, 152–165, https://doi.org/10.1061/ASCEHE.1943-5584.0000162, 2010.

Perthame, B. and Simeoni, C.: A kinetic scheme for the Saint-Venant system with a source term, CALCOLO, 38, 201–231, https://doi.org/10.1007/s10092-001-8181-3, 2001.

Pramanik, N., Panda, R. K., and Sen, D.: One dimensional hydrodynamic modeling of river flow using DEM extracted river cross-sections, Water Resources Management, 24, 835–852, 2010.

Preissmann, A.: Propagation des intumescences dans les canaux et rivieres, in: Premier Congres De L'Association Francaise de Calcul AFCAL, Grenoble 14 - 15 - 16, 1960, pp. 433–442, Gauthier-Villars, Paris, 1961.

Pu, J. H., Cheng, N.-S., Tan, S. K., and Shao, S.: Source term treatment of SWEs using surface gradient upwind method, Journal of Hydraulic Research, 50, 145–153, https://doi.org/10.1080/00221686.2011.649838, 2012.

Roe, P.: Approximate Riemann solvers, parameter vectors, and difference schemes, Journal of Computational Physics, 43, 357 – 372, https://doi.org/10.1016/0021-9991(81)90128-5, 1981.

Rosatti, G., Bonaventura, L., Deponti, A., and Garegnani, G.: An accurate and efficient semi-implicit method for section-averaged free-surface flow modelling, International Journal for Numerical Methods in Fluids, 65, 448–473, https://doi.org/10.1002/fld.2191, 2011.

Rossman, L. A.: Storm Water Management Model Reference Manual, Volume II - Hydraulics, Tech. Rep. EPA/600/R-17/111, US EPA Office of Research and Development, Water Systems Division, https://nepis.epa.gov/Exe/ZyPDF.cgi?Dockey=P100S9AS.pdf, 2017.

Saavedra, I., Lopez, J. L., and Garcıa-Martınez, R.: Dynamic Wave Study of Flow in Tidal Channel System of San Juan River, Journal of Hydraulic Engineering-ASCE, 129, 519–526, https://doi.org/10.1061/(ASCE)0733-9429(2003)129:7(519), 2003.

Saleh, F., Ducharne, A., Flipo, N., Oudin, L., and Ledoux, E.: Impact of river bed morphology on discharge and water levels simulated by a 1D Saint–Venant hydraulic model at regional scale, Journal of Hydrology, 476, 169–177, https://doi.org/10.1016/j.jhydrol.2012.10.027, 2013.

Sanders, B. F.: High-resolution and non-oscillatory solution of the St. Venant equations in non-rectangular and non-prismatic channels, Journal of Hydraulic Research, 39, 321–330, 2001.

Sanders, B. F., Jaffe, D. A., and Chu, A. K.: Discretization of integral equations describing flow in-nonprismatic channels with uneven beds, Journal of Hydraulic Engineering-ASCE, 129, 235–244, https://doi.org/10.1061/(ASCE)0733-9429(2003)129:3(235), 2003.

Sart, C., Baume, J. P., Malaterre, P. O., and Guinot, V.: Adaptation of Preissmann's scheme for transcritical open channel flows, Journal of Hydraulic Research, 48, 428–440, https://doi.org/10.1080/00221686.2010.491648, 2010.

Schippa, L. and Pavan, S.: Analytical treatment of source terms for complex channel geometry, Journal of Hydraulic Research, 46, 753–763, https://doi.org/10.3826/jhr.2008.3211, 2008.

Sen, D. J. and Garg, N. K.: Efficient Algorithm for Gradually Varied Flows in Channel Networks, Journal of Irrigation and Drainage Engineering-ASCE, 128, 351–357, https://doi.org/10.1061/(ASCE)0733-9437(2002)128:6(351), 2002.

Szymkiewicz, R.: Finite-Element Method For The Solution Of The Saint Venant Equations In An Open Channel Network, Journal Of Hydrology, 122, 275–287, https://doi.org/10.1016/0022-1694(91)90182-H, 1991.

Tucciarelli, T.: A new algorithm for a robust solution of the fully dynamic Saint-Venant equations, Journal of Hydraulic Research, 41, 2003.

Vazquez-Cendon, M.: Improved treatment of source terms in upwind schemes for the shallow water equations in channels with irregular geometry, Journal of Computational Physics, 148, 497–526, 1999.

Venutelli, M.: Stability and accuracy of weighted four-point implicit finite difference schemes for open channel flow, Journal of Hydraulic Engineering-ASCE, 128, 281–288, https://doi.org/10.1061/(ASCE)0733-9429(2002)128:3(281), 2002.

Venutelli, M.: A fractional-step Padé Galerkin model for dam-break flow simulation, Applied Mathematics and Computation, 134, 2003.

Venutelli, M.: A third-order explicit central scheme for open channel flow simulations, Journal of Hydraulic Research, 44, 402–411, 2006.

Wang, G.-T., Yao, C., Okoren, C., and Chen, S.: 4-Point FDF of Muskingum method based on the complete St Venant equations, Journal of Hydrology, 324, 339–349, https://doi.org/10.1016/j.jhydrol.2005.10.010, 2006.

Wang, J., Ni, H., and He, Y.: Finite-difference TVD scheme for computation of dam-break problems, Journal Of Hydraulic Engineering-ASCE, 126, 253–262, https://doi.org/10.1061/(ASCE)0733-9429(2000)126:4(253), 2000.

Wood, E. F., Roundy, J. K., Troy, T. J., van Beek, L. P. H., Bierkens, M. F. P., Blyth, E., de Roo, A., Doll, P., Ek, M., Famiglietti, J., Gochis, D., van de Giesen, N., Houser, P., Jaffe, P. R., Kollet, S., Lehner, B., Lettenmaier, D. P., Peters-Lidard, C., Sivapalan, M., Sheffield, J.,

Wade, A., and Whitehead, P.: Hyperresolution global land surface modeling: Meeting a grand challenge for monitoring Earth's terrestrial water, Water Resources Research, 47, 1–10, 2011.

Wu, W. M. and Wang, S. S. Y.: One-dimensional Modeling of dam-break flow over movable beds, Journal of Hydraulic Engineering-ASCE, 133, 48–58, https://doi.org/10.1061/ASCE0733-94292007133:148, 2007.

Wu, W. M., Vieira, D. A., and Wang, S. S. Y.: One-dimensional numerical model for nonuniform sediment transport under unsteady flows in channel networks, Journal of Hydraulic Engineering-ASCE, 130, 914–923, https://doi.org/10.1061/(ASCE)0733-9429(2004)130:9(914), 2004.

Xing, Y.: Exactly well-balanced discontinuous Galerkin methods for the shallow water equations with moving water equilibrium, Journal of Computational Physics, 257, 536–553, https://doi.org/10.1016/j.jcp.2013.10.010, 2014.

Xing, Y. and Shu, C.-W.: High-order finite volume WENO schemes for the shallow water equations with dry states, Advances In Water Resources, 34, 1026–1038, https://doi.org/10.1016/j.advwatres.2011.05.008, 2011.

Xing, Y. and Zhang, X.: Positivity-Preserving Well-Balanced Discontinuous Galerkin Methods for the Shallow Water Equations on Unstructured Triangular Meshes, Journal Of Scientific Computing, 57, 19–41, https://doi.org/10.1007/s10915-013-9695-y, 2013.

Ying, X. and Wang, S. S. Y.: Improved implementation of the HLL approximate Riemann solver for one-dimensional open channel flows, Journal of Hydraulic Research, 46, 21–34, 2008.

Ying, X., Khan, A. A., and Wang, S. S. Y.: Upwind Conservative Scheme for the Saint Venant Equations, Journal of Hydraulic Engineering-ASCE, 130, 977–987, https://doi.org/10.1061/(ASCE)0733-9429(2004)130:10(977), 2004.

Zeng, W. and Beck, M. B.: STAND, a dynamic model for sediment transport and water quality, Journal of Hydrology, 277, 125–133, https://doi.org/10.1016/S0022-1694(03)00073-8, 2003.

Zhu, D. J., Chen, Y. C., Wang, Z. Y., and Liu, Z. W.: Simple, Robust, and Efficient Algorithm for Gradually Varied Subcritical Flow Simulation in General Channel Networks, Journal of Hydraulic Engineering-ASCE, 137, 766–774, https://doi.org/10.1061/(ASCE)HY.1943-7900.0000356, 2011.